THE ROLE OF CFP1 IN MAINTAING LIVER HOMEOSTASIS IN A MURINE MODEL

by

Nandita Chittajallu

A Thesis

Submitted to the Faculty of Purdue University

In Partial Fulfillment of the Requirements for the degree of

Master of Science

Department of Biological Sciences

Indianapolis, Indiana

August 2017

THE PURDUE UNIVERSITY GRADUATE SCHOOL
STATEMENT OF COMMITTEE APPROVAL

Dr. David G. Skalnik, Chair
Department of Biology
Dr. Guoli Dai
Department of Biology
Dr. Nicolas F. Berbari
Department of Biology

Approved by:

Dr. James A. Marrs
Head of the Graduate Program

ACKNOWLEDGMENTS

Firstly, I would like to acknowledge the pivotal role of my mentor, Dr. David Skalnik who provided me with the opportunity to grow as a scientist by allowing me the opportunity to achieve my Master's degree in his lab. Through his mentorship, I was able to acquire scientific skills that will continue to benefit me in the future. I am so grateful to him for his unwavering patience, support, and belief in me over the past two years.

I am grateful for the support, guidance, and friendship of my former lab members. Erika Dobrota took me under her wing from the moment that I entered the lab and I will forever treasure our friendship and the memories we shared. She was a constant source of support and guidance both inside and outside of the laboratory over the past two years. I would also like to thank my two undergraduate students, Shelby Canella and Morgan Murray, who put in countless hours helping me bring my project to fruition. They were both dedicated, intelligent women and I'm so grateful that they provided me the opportunity to mentor them.

I would also like to thank the staff of the Biology Department. I am honored to have been able to work closely with many of them and to have learned so much from them. I would especially like to thank Dr. Simon Atkinson, Dr. Stephen Randall, and Dr. Guoli Dai for being remarkable professors who truly cared about their students. I would also like to thank Dr. Guoli Dai for his integral role in my thesis project as a collaborator, mentor, and friend. His kindness and support meant a great deal to me. I would like to thank Dr. Kathy Marrs, Dr. Martin Vaughan, Dr. Patrick Gentry, and Dr. Robert Yost for the opportunity to serve as a teaching assistant and their guidance throughout the experience. This opportunity allowed me to become a proficient public speaker and

presenter as well as to realize my love for teaching. I would also like to acknowledge my interactions with Dr. James Marrs, Dr. A.J. Baucum, Dr. James Meyers, and Dr. Jiliang Li for always being there with a kind word and helping hand. I would also like to recognize Sue Merrell, Shari Dowell, and Angela Longfellow for working so hard behind the scenes to ensure that everything runs smoothly.

I am so grateful to the Small Animal Research Center (SARC) staff for all of their animal husbandry advice and help as well as the close friendships I formed with many of them. I would like to thank Chris Konz for going out of his way to put me in touch with people and always being a wonderful person to be around. I'd like to thank Julie Nigro and Vickie Burge for all of their help showing me the ropes in the colony room and helping me whenever I needed an extra pair of hands. They were also great friends. I will forever remember the stories and laughter we shared together. I'd also like to thank Shanon Gibson for her cheery personality. It was always a pleasure to run into her.

The comraderie that exists between all of the graduate students in the department is remarkable. I am so grateful to all of them for always being there to answer questions, lend advice, and share a laugh. There are so many students that had an impact on me over the past two years, but I would like to especially thank Shashank Nambiar and Joonyong Lee without whom I would have been unable to complete my thesis. They patiently taught me many of the animal procedures I performed and were always available to answer any questions I had, loan me equipment, and provide guidance.

Last but not least, I would like to thank my friends and family for being my unwavering support base. I would like to thank Deborah McDonald for always giving me company and checking in on me whenever I'd have late nights in the lab. She always had

a smile and positive demeanor that helped raise my spirits. I would like to thank Amanuel Kibrom for always being there to swap ideas, provide constructive criticism, and help me be a better scientist. I would also like to acknowledge Emily Zhang and Ani Yalamanchi for their help making sense of my serum data. I'd like to thank Deshea Meely, Jenna Jones, Kevin Hinkle, Chad Nobbe, Stephanie Corona, Evan Glass, Kyle Robinson, and Lizzie Hart for giving me support from afar and Illya Moskavin, Kathleen Swilik, Ruben Solis, and Jordan and Ally Bergoetz for being part of my support network in Indy. I would like to thank Max Stillions for listening to all of my "science talk" as I drove home from the lab every day and always being there for me during the good times and the bad. Most importantly, I'd like to thank my sister, Supriya Chittajallu, and my parents, Namratha and Siva Chittajallu, for being there for me not just over the past two years but my entire life. They were there for me every step of the way and I wouldn't be even a fraction of the person I am today without them.

TABLE OF CONTENTS

LIST OF TABLES

LIST OF FIGURES

LIST OF ABBREVIATIONS

Alb	albumin
ALT	alanine aminotransferase
AST	aspartate aminotransferase
bp	base pair
C	Celsius
cc	cubic centimeter
CFP1	CXXC Finger Protein 1
CHIP-Seq	chromatin immunoprecipitation sequencing
COMPASS	Complex Proteins Associated with Set1
CpG	cytosine connected by a phosphate group to guanine
Cyp2d9	cytochrome P450 2d9
D	day(s)
dL	deciliter
DNA	deoxyribonucleic acid
DNMT	DNA methyltransferase
dNTP	deoxyribonucleoside triphosphate
ELISA	enzyme-linked immunosorbent assay
FATP5	fatty acid transporter 5
Fl	filial generation 1
fl	floxed
g	gram(s)
G1	growth phase 1
G2	growth phase 2
GH	growth hormone
H	hour(s)
H&E	haematoxylin and eosin
H2a	histone 2a
H2b	histone 2b
H3	histone 3
H3K4	histone 3 lysine 4
H3K4me	histone 3 lysine 4 methylation
H4	histone 4
het	heterozygous
HMT	histone methyltransferase
IR	insulin resistance
kg	kilogram
KRAB-ZFP	Krüppel-associated box zinc finger proteins
L	liter(s)
M	molarity
mg	milligram(s)
min	minute(s)
mL	milliliter(s)
m*M*	millimolar

mRNA	messenger RNA
Mup	major urinary protein
NAFL	non-alcoholic fatty liver
NASH	non-alcoholic steatohepatitis
nm	nanometer(s)
OCT medium	optimal cutting temperature compound
PCR	polymerase chain reaction
PH	partial hepatectomy
PHD	plant homeodomain
PTM	post-translational modification
RNA	ribonucleic acid
RNA-Seq	RNA sequencing
Rpm	revolutions per minute
RSL	regulators of sex limitation
S phase	synthesis phase
SARC	Science Animal Research Center
sdH2O	sterile distilled water
Slp	sex-limited protein
TUNEL	terminal deoxynucleotidyl transferase-mediated dUTP nick end-labeling
wt	wildtype

ABSTRACT

Author: Chittajallu, Nandita. MS
Institution: Purdue University
Degree Received: August 2017
Title: The Role of CFP1 in Maintaining Liver Homeostasis in a Murine Model
Major Professor: David Skalnik

CXXC finger protein 1 (CFP1) is an epigenetic regulator of H3K4 and cytosine methylation. Due to its role in establishing and maintaining methylation patterns, CFP1 determines whether DNA is found in its euchromatin or heterochromatin state and as such whether genes are transcriptionally active or inactive. In stem cells, deficiency of CFP1 results in inability to differentiate and in murine embryos it results in peri-implantation death. Despite the demonstrated importance in developing tissue, the role of CFP1 in mature tissues, such as the liver, has yet to be elucidated. This study examined the role of CFP1 in maintaining liver homeostasis under conditions involving hepatocellular stress by examining liver regeneration, pregnancy-induced hepatomegaly, and non-alcoholic steatohepatitis (NASH) disease progression. The liver's ability to recover was analyzed through liver:body mass ratios, blood serum analysis, liver histology, and qualitative observations. Deficiency of CFP1 in the livers of animals subjected to partial hepatectomies (PH) resulted in decreased liver regeneration capacity with liver mass restoration becoming significantly different starting at 48H post-PH and remaining so until 10D post-PH. This decreased regeneration appeared to be the result of reduced hepatocyte mitosis. Mouse dams lacking hepatic CFP1 mated with males expressing CFP1 displayed a proclivity for dystocia. Mice subjected to a fast food diet resulting in NASH while lacking hepatic CFP1 experienced decreased weight gain and

hepatic lipid accumulation compared to their CFP1 expressing counterparts. Through these three studies, the critical role of CFP1 for the maintenance of liver homeostasis was demonstrated.

CHAPTER 1. INTRODUCTION

1.1 Epigenetics

In 1956, British developmental biologist Conrad Waddington coined the term epigenetics after successfully demonstrating that environmental stimuli could affect the expression of genes without changing the underlying nucleotide sequence.[22,40] In doing so he asserted that epigenetics served as the link between the genotype and phenotype and would ultimately determine the final outcome of a gene.[22] Since its creation as a new field in science, various genetic phenomenon that diverged from the normal rules of genetics were lumped under this category. Some examples include paramutations in maize, position effect variegation in Drosophila, and imprinting of specific paternal or maternal loci in mammals.[1,22,40]

Improved technology has provided further insight into the molecular basis behind epigenetics. It is now understood to occur through covalent modifications to both DNA and its histone proteins causing changes in the chromatin structure and therefore gene expression. These changes allow for stabilization of gene expression programs and canalization of cell lineages necessary for survival.[1] These epigenetic modifications can be achieved through chemical modifications that include methylation, ubiquitination, acetylation, sumoylation, and phosphorylation of DNA and its associated histone proteins.[22]

1.2 Chromatin

One of the most easily distinguishing features differentiating eukaryotic organisms from prokaryotic organisms is their nucleus where their DNA is stored. In eukaryotic organisms, this DNA can stretch to over 1 meter long.[36] In order to store the

genetic material, eukaryotic cells package DNA into a condensed state called chromatin. Chromatin is organized into structural units called nucleosomes which consist of 146-147 bp stretches of DNA wrapped around histone protein octamers with an approximately 200 bp section of linker DNA connecting one nucleosome to the next to form an 11 nm beads-on-a-string array.[3,36]

The histone proteins that compose the histone octamer are small, positively charged proteins with numerous lysine and arginine amino acid residues.[11] The chemical constitution of the histones allows the negatively-charged DNA to wrap around them. The histone octamer is composed of two copies of H2a, H2b, H3, and H4 proteins. They are organized into one tetramer of two H3-H4 heterodimers flanked by two H2A-H2B heterodimers to form the octamer.[2,41] Despite low sequence similarity, all of the core histones contain a histone fold domain which is composed of three α-helices connected by two loops. This domain allows for heterodimeric interactions to take place via the handshake motif.[2,36]

DNA-templated processes are controlled to a high degree by the state of the chromatin. If the chromatin is in its euchromatin state where it is an 11 nm fiber loosely wrapped around the histone proteins, the transcription machinery is able to access the DNA template and produce mRNA which is then translated into proteins. If chromatin is found in its heterochromatin state, nucleosomes are packaged as a 30 nm fiber causing the transcription machinery to be unable to access the DNA template making it the transcriptionally inactive state of chromatin. Therefore the cell must make use of epigenetic factors to organize the genome into its respective chromatin state based on the probability of a gene being necessary for cellular functions.

1.3 Methylation

One of the most extensively studied forms of epigenetic modifications is cytosine methylation. Methylation is performed by DNA methyltransferases (DNMTs) which transfer methyl groups from S-adenosyl-L-methionine to the cytosine bases of eukaryotic DNA converting them to 5-methylcytosine.[9,27] In mammals there are three primary DNMTs which perform different functions. DNMT3a and DNMT3b are responsible for establishing de novo methylation patterns while DNMT1 is responsible for maintaining methylation patterns. After replication, the template strand contains the original methylation patterns, however, the nascent strand does not. DNMT1 ensures that the established patterns are passed on.[9] There is some overlap in function between these various DNMTs.[27]

Cytosine bases, which are the target of methylation, are often found next to guanine. This is termed a CpG dinucleotide because the cytosine is connected to the guanine by a phosphate group. In mammals, methylation of cytosine is usually associated with gene silencing.[32,43] Methylation is mainly concentrated to CpG dinucleotides scattered throughout the genome. The exception to this is CpG islands which are approximately 1 kilobase stretches of DNA containing high CpG concentrations. These CpG islands are unmethylated and 70% of them are found upstream of promoter sequences of many genes. Methylation of them can result in inappropriate gene silencing which can be result in cancerous cells or cell lethality.[43]

1.4 Histone Modifications

The N-terminal tails of histone proteins are subject to post-translational modifications (PTMs) which change the binding affinity to the DNA and the

conformation of the chromatin therefore affecting the chromatin state. These PTMs often occur on the basic lysine and arginine residues of the tails. These modifications can include acetylation, sumoylation, phosphorylation, ubiquitination, and methylation.[22,42] Histone methylation is the epigenetic modification of interest in this study and is performed by histone methyltransferases (HMTs). HMTs can either mono- or di-methylate arginine residues while lysine residues can be either mono-, di-, or tri-methylated.[42]

1.5 CXXC Finger Protein 1

CXXC Finger Protein 1 (CFP1) is a transcriptional activator that regulates both cytosine methylation and histone methylation. It was first discovered in mammals, however, its homolog is present in other species, such as Caenorhabditis elegans, Drosophila, Saccharomyces cerevisiae, and Schizosaccharomyces pombe. Its homolog in yeast, Spp1, is part of the histone 3 lysine 4 methylation complex known as COMPASS. Similar to Spp1, CFP1 regulates histone methylation through its role as a component of the human Set1 complexes which are responsible for the majority of the H3K4 methylation marks present throughout the genome.[31] These H3K4 methylation marks are associated with transcriptionally active euchromatin.[51] It is believed that CpG islands are responsible for recruiting H3K4 methylation as they are often found in conjunction upstream of gene promoters.[52]

CFP1 is encoded by the CXXC1 gene which is 5,980 base pairs long, found on chromosome 18, and contains various domains. It has two conserved plant homeodomains (PHD) that are associated with chromatin mediated transcription control and may be able to differentiate between histone tails with different modifications. It

contains a crescent shaped CXXC zinc finger domain which is able to fit into the major groove of the DNA in regions of unmethylated CpGs. Its Set1 interaction domain (SID) allows it to interact with the Set1 methyltransferase complexes and regulate their activity and it also contains acidic, basic, and coiled-coil domains (Figure 1.5).[59]

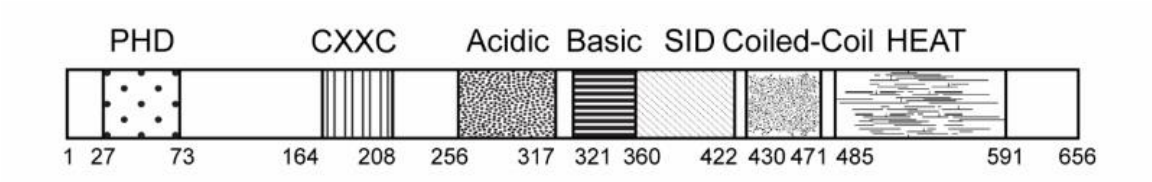

Figure 1.5. Domain Structure of CFP1

Schematic representation of the conserved domains of CFP1. The amino acid position of each domain is denoted below the figure.

1.6 CFP1 Research

Based on CFP1's role in epigenetics, it was an interesting target for knock-out experiments. In stem cells, their lineage commitment is characterized by global remodeling of chromatin structure. This remodeling allows for levels of heterochromatin to increase causing restriction of gene transcription and developmental potential. Deficiency in CFP1 caused loss of H3K4me at CGIs and mislocalization of H3K4me to heterochromatic regions.[34] In addition, a 70% reduction of global cytosine methylation and 50% reduction of DNMT1 activity was observed.[12] As a result, stem cells remain viable but unable to differentiate.

Murine embryos lacking CFP1 experience peri-implantation lethality and inability to gastrulate. They experience death between 4.5 and 6.5 days post coitom which corresponds with global changes in methylation patterns.[12] Mice homozygous for the conditional CXXC1 gene and carrying the Mx1-Cre recombinase transgene were utilized to examine the effects of CFP1 in the liver and hematopoietic systems. These animals

died between 9 to 13 days following deletion of CXXC1 and were observed to have reduced bone marrow progenitor cells and mature peripheral blood cells.[16] To further elucidate the role of CFP1 in the liver, mice were produced that were homozygous for the conditional CXXC1 gene and carried the Cre recombinase gene under the control of an albumin promoter. These mice lacked hepatic CFP1 and were viable, however, 40% of these mice died within a year and expressed a "wasting phenotype" characterized by decreased body mass, reduced vitality, and hunched posture (Figure 1.6). The livers of these mice exhibited altered H3K4me patterns and many exhibited regenerative nodules.[35]

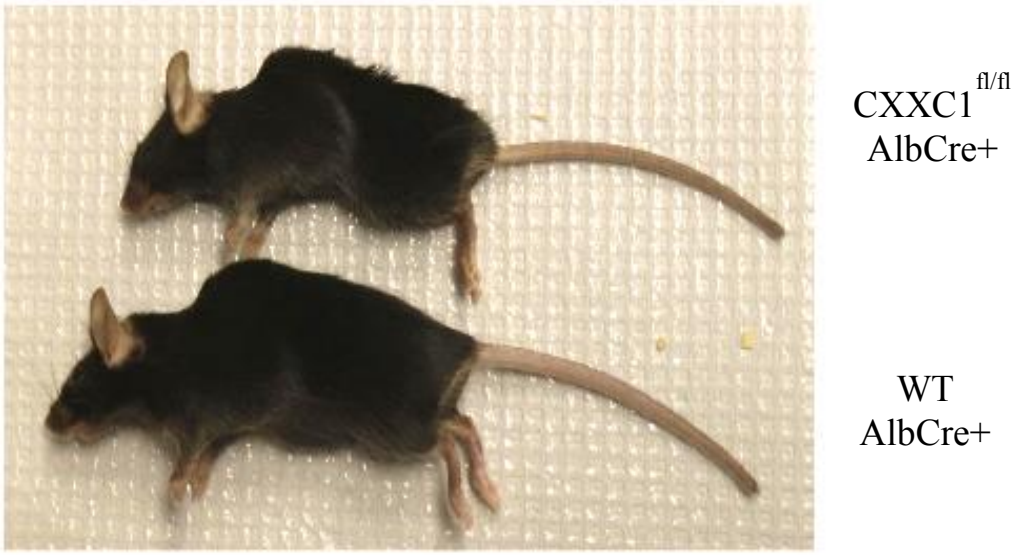

Figure 1.6. CFP1-deficient Mice Exhibited "Wasting" Phenotype

Photographic representation highlighting the differences in body size and posture between the sick CXXC1$^{fl/fl}$ AlbCre+ mouse and the normal, healthy CXXC1$^{+/+}$ AlbCre+ mouse.

1.7 Liver

The liver is a remarkable organ that performs an array of vital processes including detoxification of blood, storage and release of nutrients, production of bile, and synthesis of proteins important for blood clotting and other processes.[49] It is located below the diaphragm and composed of three lobes in humans and five in mice. These lobes are provided with nutrients and oxygenated blood via two major blood vessels: the portal vein and hepatic artery.

The cells that the liver is composed of come from both parenchymal and nonparenchymal origins. The parenchymal cells of the liver originate from hepatoblasts which are the bipotential stem cells of the liver. They can differentiate into either hepatocytes or cholangiocytes. The hepatocytes are the functional unit of the liver and constitute 80% of the liver volume. Cholangiocytes are the epithelial cells that line the bile ducts. The non-mesenchymal cells of the liver include Kupffer cells, stellate cells, and endothelial cells.[49] The Kupffer cells are macrophages of liver which aid in the detoxification of the blood. The stellate cells are responsible for collagen deposition and are associated with fibrosis. They are also the major storage site of Vitamin A in the body.[58]

Within the liver lobes, cell populations are organized into structural units called lobules. The lobules are characterized by rows of hepatocytes lining the central vein. Transfer of nutrients and oxygen is facilitated by small capillaries called sinusoids which are found between the rows of hepatocytes and which drain into the central vein which eventually feeds into the hepatic vein. The sinusoids are lined by the Kupffer cells and

sinusoidal endothelial cells and stellate cells are found in the space between the sinusoids and the hepatocytes.

1.8 Liver Regeneration

The liver is intriguingly the only mammalian visceral organ capable of regeneration upon chemical or mechanical damage. This regeneration can occur via three different modes: replication of existing mature, normally quiescent hepatocytes, differentiation of oval cells which act as bipotential stem cells, or production by bone marrow cells.[21,23,29] There is a great deal of data supporting the first two modes of regeneration, however, there is little information regarding the extent to which bone marrow cells can regenerate hepatocytes or the mechanisms by which they do so.[21] Replication of mature hepatocytes is the preferred mode of regeneration due to its speed and efficiency. However, when liver damage is severe or the hepatocytes are not able to replicate due to senescence or arrest, oval cell differentiation can serve as a compensatory mechanism.[21,46]

1.9 Partial Hepatectomy

Analysis of the cellular organization of mouse livers has shown remarkable similarity to other mammalian species and therefore it serve as a useful model species for studying mammalian liver morphology, processes, and diseases.[49] Mouse partial hepatectomy (PH) models in which ⅔ of the liver is resected have been successfully utilized to study the mechanisms by which the liver regenerates. This model is both reproducible and simple and results in robust proliferation without inflammation or massive necrosis.[46,61] PH experiments have also been beneficial in providing insight into

the genomic and epigenomic changes essential for mature, quiescent hepatocytes to re-enter the cell cycle allowing for regeneration to occur.

Past studies examining gene profiles after PH during G1, S, and G2 phases have shown that early on there is a decrease in the expression of genes that are involved in normal liver functioning such as steroid and lipid metabolism and hormone biosynthesis.[46] During G1 and continuing into S-phase, there is an upregulation of genes necessary for cytoskeletal organization and protein synthesis. Between 4 and 12 hours after the surgery, a transcriptional shift occurs in the mature hepatocytes which prepares them for re-entering the cell cycle. Transcription regulatory factors such as FOXD3, FOXI1, CUX1, ER, and E2F-1 are activated by 4 hours post-surgery until around 12 hours post-surgery. At this point, genes associated with DNA replication are activated in the hepatocytes in preparation for the decision to replicate.[46]

Hepatocyte replication occurs in four waves with approximately 24 hours between two adjacent mitosis peaks. The first wave lasts from 24 to 60 hours post-PH. The second wave is from 60 to 84 hours post-PH. The third wave is from 84 to 108 hours post-PH and the fourth wave is from 108 to 132 hours post-PH. With each successive wave, the amount of hepatocytes regenerating decreases as the number of cells gets closer to the unperturbed liver state. The first wave is the most robust with the highest number of remaining hepatocytes entering into the cell cycle. The combined number of hepatocytes replicating in the second and third waves is equivalent to the number in the first wave. The fourth wave is minor. Liver mass is restored by 7 to 10 days after the injury.[61]

1.10 Maternal Liver

During pregnancy many maternal organs experience changes in their structure and function in order to compensate for the needs of the developing fetus and placenta. These organs include but are not limited to the brain, cardiovascular system, pancreas, immune system, and liver. Hepatomegaly is crucial during pregnancy because it makes it possible for the liver to support the increased metabolic load placed on the mother.[37]

In mice, gestation lasts for 18 to 22 days, and by day 18 of pregnancy the maternal liver doubles in size when compared to the non-pregnant state. This dramatic expansion in size is believed to occur through both hypertrophy meaning increased cell size and hyperplasia meaning increase in cell number.[37,61] Analysis of gene expression has revealed some overlap in the molecular mechanisms utilized by the liver during injury-induced hepatocyte proliferation and pregnancy-induced proliferation. IL-6, TNF1α, NFkB, c-Jun, and IL-1β were found to be activated due to the pregnancy-induced liver growth, however, HGF, FGF1, TNFR1, CAR, and PXR were unaffected. In addition, hepatic STAT3, β-catenin, and EGFR were activated, however hepatic c-Met was not.[61]

1.11 NASH Animal Model

As chronic overnutrition and obesity rise, diseases like metabolic syndrome increase in prevalence. In the liver, metabolic syndrome manifests as non-alcoholic fatty liver disease (NAFL).[54] NAFL is currently one of the leading causes of liver disease worldwide with a prevalence of 30% in adults in the United States general population.[7] It is differentiated from alcoholic fatty liver disease by the distinction that in NAFL, hepatic

macrovesicular steatosis occurs under conditions where the individual ingests less than 20 g of alcohol per day.[53]

Non-alcoholic steatohepatitis (NASH) is the progression of NAFL that occurs in between 5.7%–17% of the general population.[53] It is one of the leading causes of cirrhosis and one of the major reasons for liver transplants in the United States.[33] Histologically, it is characterized by progressive fibrosis and hepatocellular ballooning.[13]

Recently a model for NASH was created in order to gain insight into this disease. It was created by feeding mice a diet high in fat, cholesterol, and fructose. This differs from the Western diet which was able to create NASH with the presence of fibrosis markers but due to the absence of fructose was unable to produce hepatocyte injury in the form of cellular ballooning.[13,48]

CHAPTER 2. METHODS

2.1 Generation of CXXC1$^{fl/fl}$ AlbCre+/- Line of Mice

Male CXXC1$^{fl/fl}$ AlbCre+ mice generated by Jyothi Mahadevan, utilizing the cre-lox system, were initially mated with female C57BL/6 mice from Jackson Laboratories due to a lack of female mice with the desired genotype.[36] The offspring of this cross were heterozygous for the CXXC1 allele (CXXC1$^{fl/wt}$) with half of them carrying the Cre transgene. Crosses were then set up of CXXC1$^{fl/wt}$ individuals with one individual of each pair carrying the Cre transgene. Once CXXC1$^{fl/fl}$ mice were generated, male CXXC1$^{fl/fl}$ mice carrying the Cre transgene were mated with female CXXC1$^{fl/fl}$ lacking the Cre transgene which resulted in all of the offspring being homozygous for the floxed CXXC1 allele and half of them carrying the Cre transgene.

2.2 Genomic DNA Isolation

At 3 weeks of age, mouse pups were weaned and tail snipped using the approved SARC protocol. If snips needed to be collected after three weeks of age, the mice were briefly anesthetized using a 2% flow of isofluorane and an oxygen flow rate of 0.8 L/min. In order to extract DNA from the snips, 600 µL of cell lysis buffer (10 mM Tris [pH 8.0], 100 mM EDTA, 0.5% SDS) and 10 µL of Proteinase K (20 mg/mL) were added to the tubes containing the tissue. They were then placed in a 50°C water bath overnight to allow for tissue digestion to occur. Following this, the digests were incubated with 6 µL of RNase A (10 mg/mL) in a 37°C water bath for 15 minutes. 200 µL of 7.5 M ammonium acetate was added and then the tubes were vortexed for 30 seconds and placed on ice for 10 minutes. They were centrifuged at 4°C for 30 minutes at 13,000 rpm in order to pellet proteins and extracellular debris. 750 µL of the supernatant was placed

in fresh tubes before adding 525 µL isopropanol. The tubes were then inverted to mix the contents and centrifuged at room temperature for 2 minutes at 13,000 rpm to pellet the isolated DNA. The supernatant was discarded and the DNA was washed with 500 µL of 70% ethanol. The tubes were centrifuged at room temperature for 1 minute at 13,000 rpm and the supernatant was discarded. The pellets were allowed to air dry and then re-suspended in 50 µL of sdH2O.

2.3 Genotyping

Amplification of the DNA acquired from the tail snips was achieved through PCR. Two 50 µL reaction mixtures were created for each sample containing 0.5 µL of template DNA from the tail snips, 1 µL of the forward primer, 1 µL of the reverse primer, 0.25 µL of Econo Taq Polymerase, 0.4 µL of dNTP, and 41.95 µL of distilled water. The primers for indicating whether an individual was $CXXC1^{fl/fl}$ were CONS2 (TGT AGA CAC TTG TGG GAA GCC) and SRLH23 (AGT TCA CCC AGA CCC TCT TCC). The primers indicating the presence of the Cre-recombinase were oIMR 1084 (GCG GTC TGG CAG TAA AAA CTA TC) and oIMR1085 (GTG AAA CAG CAT TGC TGT CAC TT).

They were then run in a thermocycler using the following conditions: initial denaturation at 95°C for 4 minutes followed by 31 cycles of 95°C for 4 minutes, 62°C for 45 seconds, and 72°C for 45 seconds. The final elongation was at 72°C for 5 minutes and the final hold was 4°C after which the amplified product was either stored at 4°C or prepared for gel electrophoresis by adding 10 µL loading dye. A 1.2% agarose gel was prepared using 1x TBE (108 g Tris base, 55 g Boric acid, 40 mL of 0.5 EDTA [pH 8.0], distilled water), 1.2 g of agarose, and 2 µL of ethidium bromide. The bands were visualized using ultraviolet light.

2.4 Partial Hepatectomy

Male and female CXXC1$^{fl/fl}$ AlbCre+ and CXXC1$^{fl/fl}$ AlbCre- aged 3-6 months old were subjected to partial hepatectomies. The surgeries were performed by Dr. Guoli Dai from the Department of Biology, IUPUI, using a previously published protocol. Mice were briefly anesthetized and weighed and then re-anesthetized for the surgery using a 2% flow of isofluorane and an oxygen flow rate of 0.8 L/min. They were placed on a hot pad in order to prevent hypothermia. The upper abdomen was sterilized by spraying with 70% ethanol and then a midline incision was made just below the rib cage to make the liver visible. The three anterior lobes (left lateral lobe, left median lobe, and right median lobes) were ligated at the lobe origins and then resected. Notes regarding the gallbladder and any health conditions were noted and recorded. Any mice experiencing poor health conditions such as kidney tumors and malocclusions were removed from the study. Following the partial hepatectomy, the peritoneum was closed using 2-0 silk suture and the skin was closed using wound closure clips. A 3.0 cc shot of saline was delivered subcutaneously to promote recovery and then the mice were placed under a heat lamp for 15 minutes to keep them warm as they woke up from the anesthesia.

2.5 Generation of NASH CXXC1$^{fl/fl}$ AlbCre+/- Line of Mice

Male CXXC1$^{fl/fl}$ AlbCre+ and CXXC1$^{fl/fl}$ AlbCre- aged 1.5-3 months were placed on a fast food diet (23% fat, 30% fructose, and 20,000ppm cholesterol). Several male mice of both genotypes were given the LabDiet Laboratory Rodent Diet to serve as controls. All of these mice were single-housed in order to promote a more sedentary lifestyle in accordance with previous work.[13] Each of the mice were weighed weekly to monitor weight increase and ensure that the diet was not causing unintended health

consequences, such as malocclusions. Mice that experienced ulcerative dermatitis were treated with Silvadeen cream and their front and rear nails were trimmed to minimize damage done by scratching. Any mice that experienced dramatic weight reductions and poor health were sacrificed.

2.6 Tissue Collection

Tail snips and liver and blood serum samples were collected from the mice subjected to the fast food diet and partial hepatectomies as well as several untreated mice to serve as a baseline. The mice from the fast food experiments were sacrificed after 7 and 9 months (±2 days). The mice from the partial hepatectomies experiment were sacrificed at the following time points post-partial hepatectomy: 0H, 24H, 36H, 48H, 72H, 5D, and 10D. Each of the 24H, 36H, 48H, and 72H post-partial hepatectomy mice were weighed an hour prior to the sacrifice and given an intraperitoneal injection of BrdU (10 mg/ml of saline) with a dosage of 100 mg/kg of body weight. To maximize the amount of blood collected, decapitation was performed and blood was collected from the stump. The mouse was then weighed to determine the total body weight. A midline incision was made below the rib cage in order to remove the liver. Notes regarding the animal's gallbladder and any health conditions were noted. Any mice experiencing poor health conditions unrelated to the liver health were removed from the study. The liver was then removed from the body cavity.

The full liver was weighed and recorded for the fast food mice and untreated partial hepatectomy mice. The left lateral lobe and the right lateral lobe were isolated and cut into quarters. One medial quarter from the left lateral lobe was stored in 10% neutral buffered formalin (100 mL 37% formaldehyde, 900 mL distilled water, 4.0 g NaH_2PO_4,

6.5 g Na2HPO4). The other medial quarter from the left lateral lobe was covered with OCT medium and allowed to freeze by placing in a weigh boat filled with heptane sitting on dry ice. The samples were then stored at -80°C. The remaining lateral quarters were placed in separate Eppendorf tubes and the right lateral lobe was divided evenly between said tubes. The tube was then flash frozen in liquid nitrogen and stored at -80°C.

For the partial hepatectomy mice, the remnants of the ligated lobes were removed and the remaining lobes were weighed and recorded. The right lateral lobe and caudate lobe were isolated and cut into quarters. The right lateral lobe was processed using the same method as described above for the left lateral lobe and the caudate lobe was processed in the same manner as the right lateral lobe.

The tail snips were genotyped to ensure that the mice were the expected genotype. The blood was allowed to coagulate for 30 minutes following collection and then the serum was collected in a fresh Eppendorf tube and centrifuged to pellet out any remaining red blood cells. The serum was then collected in a new Eppendorf tube and then stored at -80°C.

2.7 Timed Pregnancy Breeding Scheme

Two female CXXC1$^{fl/fl}$ AlbCre- mice were mated with CXXC1$^{fl/fl}$ AlbCre+ mice to serve as controls as these animals have been shown to exhibit no fertility problems. Four female CXXC1$^{fl/fl}$ AlbCre+ females were mated with four C57 BL/6 males and two CXXC1$^{fl/fl}$ AlbCre+ females were mated with two CXXC1$^{fl/wt}$ AlbCre- males to determine if pup genotype was a factor to be considered. Ten female CXXC1$^{fl/fl}$ AlbCre+ mice were mated with CXXC1$^{fl/fl}$ AlbCre- mice to explore the potential of fertility problems upon maternal hepatic CFP1-deficiency.

2.8 Timed Pregnancy Breeding Scheme

Male and female mice were placed in the same cage between 4:00 PM and 7:00 PM and the next morning between 8:00 AM to 10:00 AM, the males were removed from the breeding cages and housed individually. The females were inspected for a mating plug. Females lacking mating plugs had this process repeated daily until a mating plug was found. Each day the female mice were weighed in order to assess via weight gain whether the pregnancy was progressing. Due to a notable amount of dystocia cases, a second round of matings utilizing the same methods was performed where the female mice were not weighed or handled during the course of the pregnancy. This was done to ensure that stress from handling was not causing additional stress on the animals resulting in health problems.

2.9 Tissue Analysis

Blood serum samples from the 0H, 48H, 5D, and 10D post-PH mice were analyzed by the IU Health Pathology Laboratory. The blood serum samples from the animal in the fast food diet study were also analyzed. They were subjected to a Hepatic Function Panel, Triglyceride Serum Quantification Panel, and Cholesterol Serum Quantification Panel in order to gain insight regarding the liver's health. These tests provided information regarding the levels of the following biochemical molecules: aspartate aminotransferase (AST), alanine aminotransferase (ALT), albumin, cholesterol, triglycerides, total protein, alkaline phosphatase, bilirubin direct, and bilirubin total.

Haematoxylin and eosin (H&E) staining was done by the IU Health Pathology Laboratory to formalin-fixed liver samples to visualize hepatocyte morphology.

Histological analysis of the slides was performed by Dr. Romil Saxena, IU Health Pathology Laboratory.

2.10 Statistical Analysis

Statistical analysis was performed on all of the data presented in this thesis by means of unpaired, one- and two-tailed t-tests with unequal variance. A difference of p-value ≤ 0.05 was designated as statistically significant. The standard error of the mean (SEM) was calculated and used for the error bars in all graphs. All statistical analysis and calculations were performed using Microsoft Excel.

CHAPTER 3. RESULTS

3.1 Effect of CFP1-Deficiency on Unperturbed Liver

The CXXC1$^{fl/fl}$ AlbCre+ male mice had a significantly ($p \leq 0.01$) smaller liver:body ratio in comparison to the CXXC1$^{fl/fl}$ AlbCre- male mice under normal, baseline conditions. CXXC1$^{fl/fl}$ AlbCre+ male mice had an average liver:body ratio of 4.49% with a corresponding value in CXXC1$^{fl/fl}$ AlbCre- male mice of 5.14%. Both CXXC1$^{fl/fl}$ AlbCre+ and CXXC1$^{fl/fl}$ AlbCre- male mice differed significantly from females of the same genotype. The liver:body ratios of CXXC1$^{fl/fl}$ AlbCre+ females did not differ significantly with CXXC1$^{fl/fl}$ AlbCre- female mice. CXXC1$^{fl/fl}$ AlbCre+ females had an average liver:body ratio of 3.94% with a corresponding value of 4.217% in CXXC1$^{fl/fl}$ AlbCre- females.

Prior work by Jyothi Mahadevan highlighted the presence of enlarged, degenerating hepatocytes as a distinguishing characteristic of the mice with CFP1-deficient livers.[35] These enlarged cells with pale cytoplasms were observed in both the male and female livers. Intriguingly there was a higher prevalence of these cells found in the female with hepatic CFP1-deficiency in comparison to their male counterparts (Figure 3.1).

Figure 3.1

Liver Histology under Unperturbed State

A. Untreated male mice (n=5, 6) were sacrificed between the ages of approximately 3 to 5 months. Their livers were harvested and preserved in 10% neutral buffered formalin until H&E staining was performed. Slides were imaged at 40x and 100x magnification. Staining showed the presence of enlarged hepatocytes with pale cytoplasms in the CXXC1$^{fl/fl}$ AlbCre+ mice.

B. Untreated females (n=5) were sacrificed at approximately 3 months old. Their livers were harvested, preserved, and imaged in the same manner as the male livers. Staining indicated the presence of enlarged hepatocytes with pale cytoplasms. There was a higher frequency of these enlarged cells present in the female CXXC1$^{fl/fl}$ AlbCre+ mice in comparison with the male CXXC1$^{fl/fl}$ AlbCre+ mice.

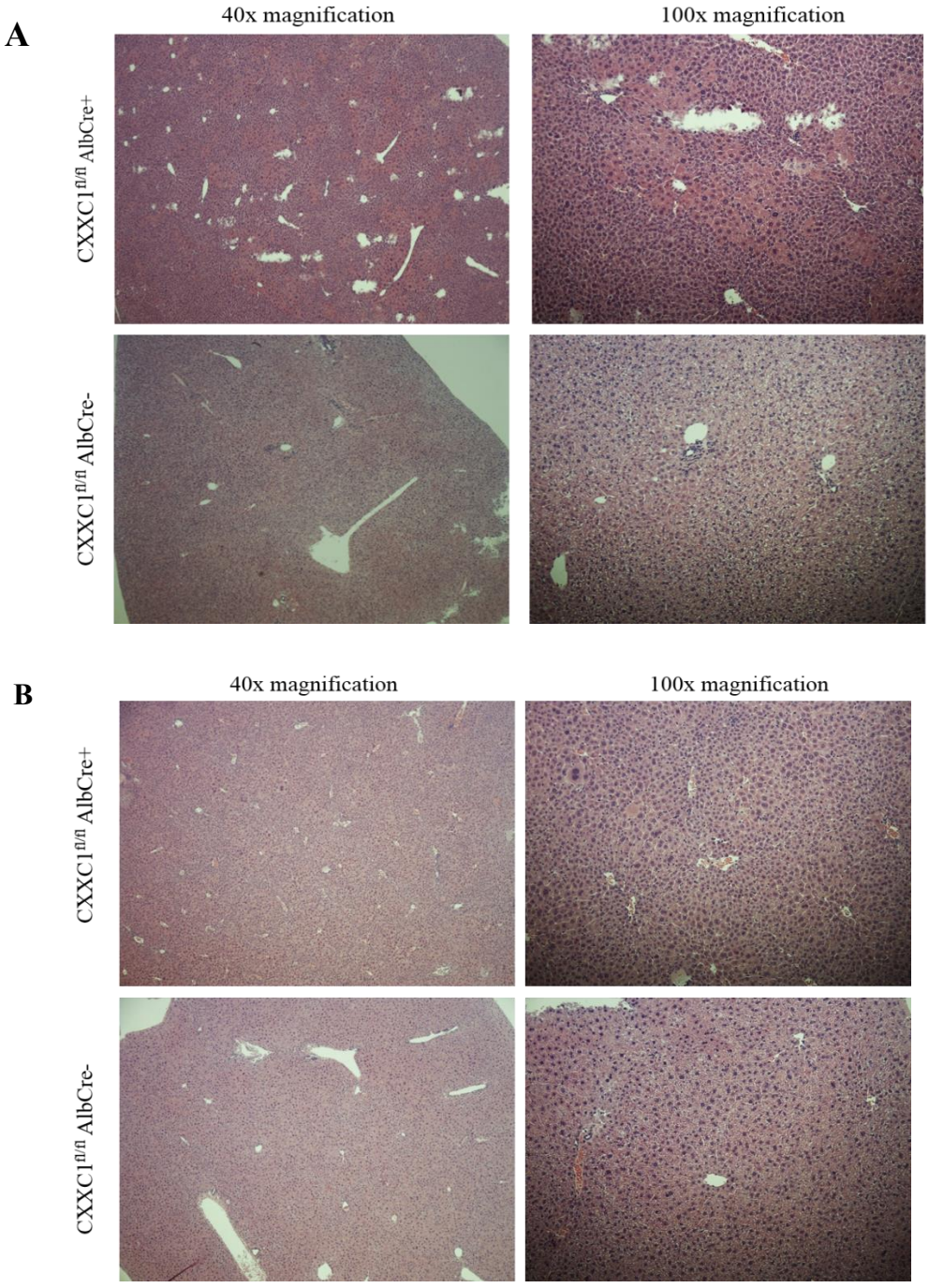
A
40x magnification
100x magnification
CXXC1fl/fl AlbCre+
CXXC1fl/fl AlbCre-
B
40x magnification
100x magnification
CXXC1fl/fl AlbCre+
CXXC1fl/fl AlbCre-

3.2 Effect of CFP1-Deficiency on Unperturbed Liver

The CXXC1$^{fl/fl}$ AlbCre- female mice mated with CXXC1$^{fl/fl}$ AlbCre+ males successfully conceived and reared pups as had been previously demonstrated in the animal colony. In addition, the CXXC1$^{fl/fl}$ AlbCre+ females that were mated with C57 BL/6 males and CXXC1$^{fl/wt}$ AlbCre- males were also able to successfully conceive and rear pups. Several litters did not survive until weaning but this is typical for first time mothers and has been observed in CXXC1$^{fl/fl}$ AlbCre- female and CXXC1$^{fl/fl}$ AlbCre+ male matings. Interestingly CXXC1$^{fl/fl}$ AlbCre+ female mice mated with CXXC1$^{fl/fl}$ AlbCre- experienced drastically decreased ability to deliver pups. In an effort to ensure that added stressors such as handling were not affecting their fertility, a second round of breedings was performed without any handling or weighing. However, the results from the second round did not show any difference in the results. 60% of these females were unable to successfully deliver the pups due to dystocia which in most cases resulted in death of both the female and pups. The likelihood of dystocia could be predicted based on changes in the female's body posture in the last few days of gestation. The dystotic females would appear more angular rather than exhibiting the swollen abdomen characteristic of normal pregnancy conditions.

3.3 Deficiency of Hepatic CFP1 in Male Mice Caused Diminished Liver Regeneration Post-PH

Liver:body ratio was calculated by dividing the liver weight by the total body weight at time of death. This was averaged for all individuals at the given time point with the same genotype in order to determine trends. The data revealed that both groups underwent liver regeneration, however, CXXC1$^{fl/fl}$ AlbCre+ animals had a much slower

rate of regeneration when compared to the CXXC1$^{fl/fl}$ AlbCre- animals (Figure 3.3). Statistical analysis showed there was no significant difference between liver:body ratios of CXXC1$^{fl/fl}$ AlbCre+ and CXXC1$^{fl/fl}$ AlbCre- animals at 0H, 24H, and 36H post-PH. However, by 48 hours and 72H, a significant difference ($p \leq 0.05$) was observed and this difference continued to increase at days 5 and 10 post-PH with a significance of $p \leq 0.01$. As noted earlier, under normal conditions liver mass is restored after 7-10 days making the observation of a significant difference between the CXXC1$^{fl/fl}$ AlbCre+ and CXXC1$^{fl/fl}$ AlbCre- at 10 days post-PH notable.

Figure 3.3. CFP1-deficient Mice Experienced Decreased Liver Regeneration Over Time

A. Male mice (n = 5,6) between the age of approximately 3 to 6 months were subjected to partial hepatectomies and then sacrificed at various time points following the partial hepatectomy. The total body weight and the liver mass were measured at the time of death. The liver:body ratio was calculated based on these measurements. A graph was constructed to display the liver:body ratio percentage for both genotypes at each of the time points studied. The blue line represents the $CXXC1^{fl/fl}$ AlbCre- mice and the orange line represents the $CXXC1^{fl/fl}$ AlbCre+ mice. The difference between the $CXXC1^{fl/fl}$ AlbCre+ and $CXXC1^{fl/fl}$ AlbCre- data points increases over time with significance denoted by asterisks. One asterisk signifies $p<0.05$ and two signifies $p<0.01$ significant.

B. A graph was constructed to display the percent of liver:body ratio percent of the baseline for both genotypes at the time points studied. These values were derived by dividing the liver:body ratio percentage by the baseline liver:body ratio percentage. Asterisks denoted significance with one asterisk signifying $p<0.05$ and two signifying $p<0.01$. Based on this analysis, the only significant time point is 5 days suggesting $CXXC1^{fl/fl}$ AlbCre+ regeneration occurs at a delayed rate.

A

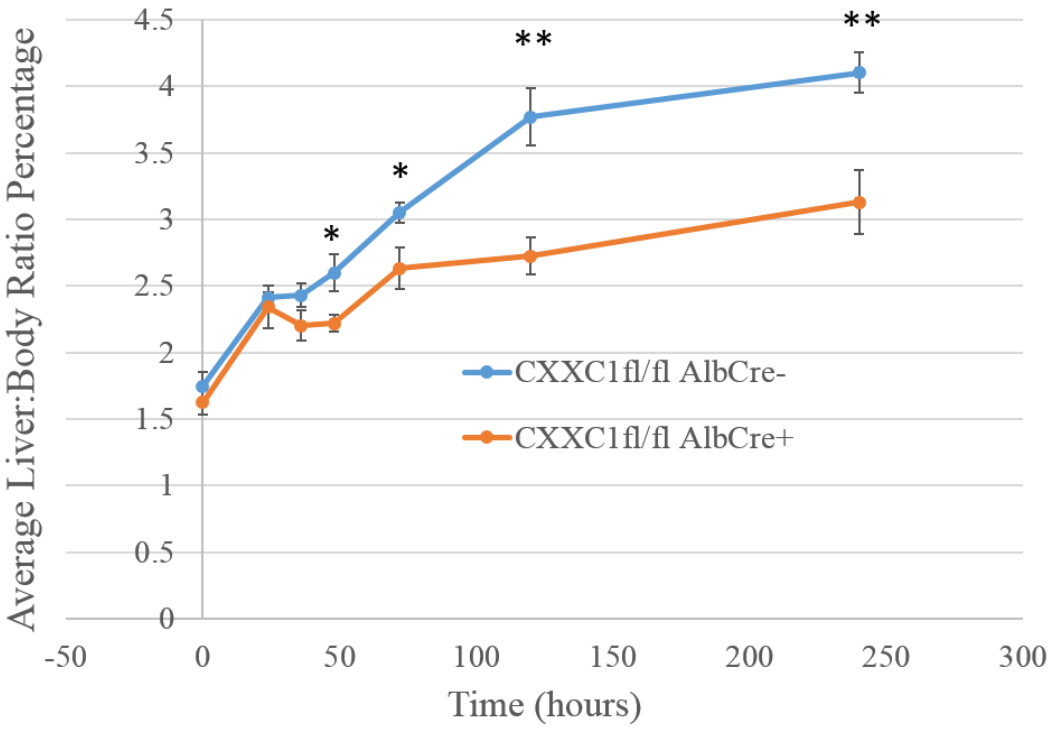
Average Liver:Body Ratio Percentage
4.5
4
3.5
3
2.5
2
1.5
1
0.5
0
-50
0
50
100
150
200
250
300
Time (hours)
**
**
*
*
CXXC1fl/fl AlbCre-
CXXC1fl/fl AlbCre+

B

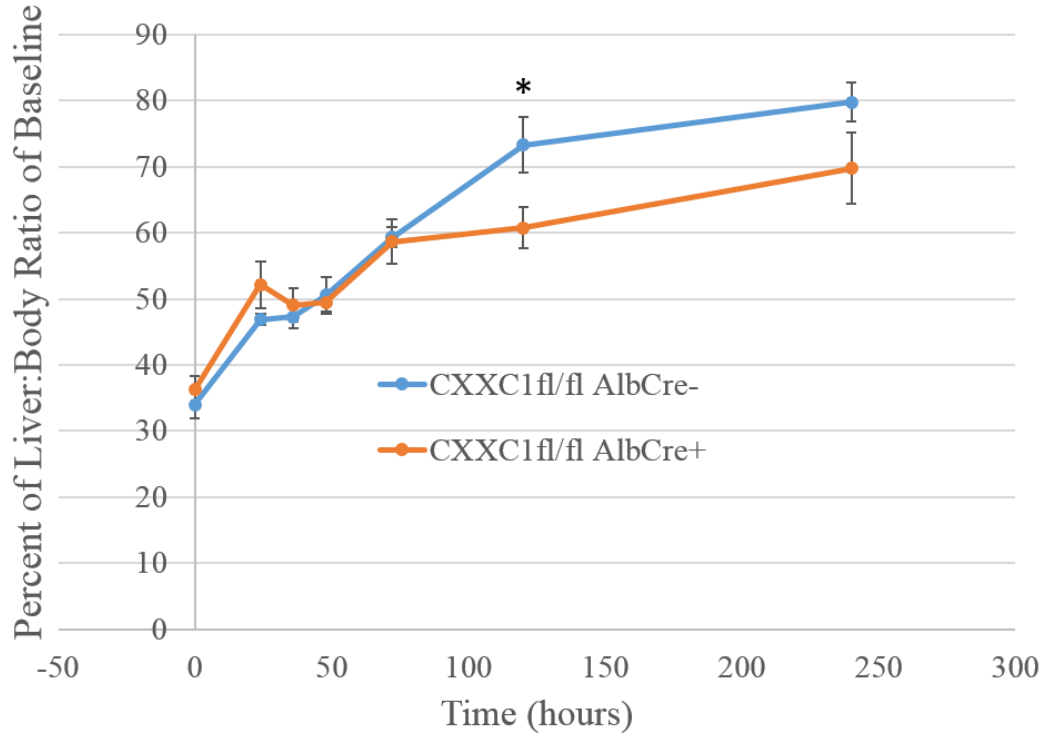
Percent of Liver:Body Ratio of Baseline
90
80
70
60
50
40
30
20
10
0
-50
0
50
100
150
200
250
300
Time (hours)
*
CXXC1fl/fl AlbCre-
CXXC1fl/fl AlbCre+

3.4 Male Gallbladder Phenotype Exhibits Variations Based on Genotype

While performing the dissections, an intriguing observation was made regarding the gallbladders. The CXXC1$^{fl/fl}$ AlbCre+ animals in the PH experiments exhibited enlarged, bile-filled gallbladders at a higher frequency than the CXXC1$^{fl/fl}$ AlbCre- animals at all of the time points post-PH (Figure 3.4). The frequency of enlarged gallbladders between the two genotypes was significantly different ($p \leq 0.01$) with a frequency of 45.71% for the CXXC1$^{fl/fl}$ AlbCre+ animals and 20.00% for the CXXC1$^{fl/fl}$ AlbCre- animals.

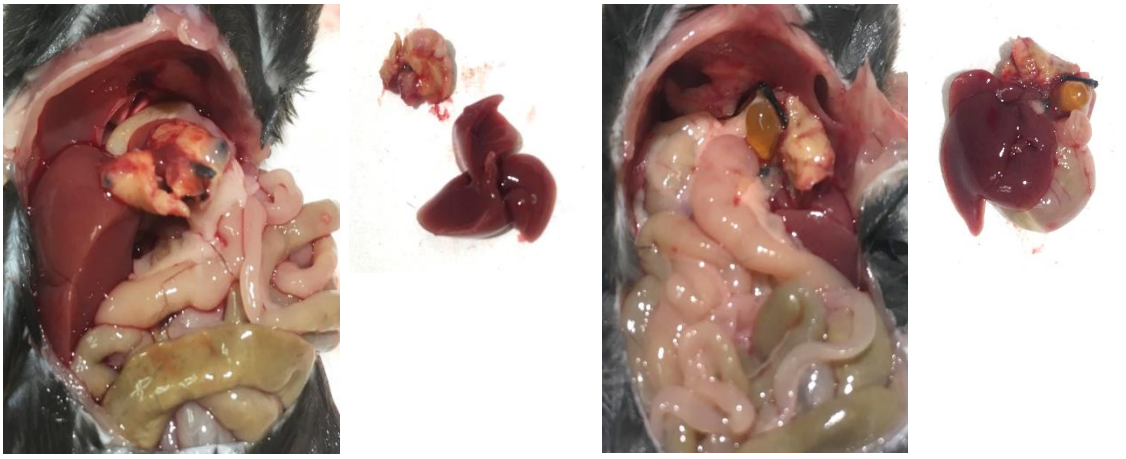

Figure 3.4. Phenotypic Difference in Gallbladders Due to CFP1-Deficiency

Photographic representation showing the enlarged, bile-filled gallbladder of a CXXC1$^{fl/fl}$ AlbCre+ male at 5D post-PH contrasted with the empty gallbladder of a CXXC1$^{fl/fl}$ AlbCre- male at the same time point. This phenotypic difference was observed at all time points examined.

3.5 Blood Serum Analysis on Post-PH Male Mice

In response to hepatocellular injury and death, phospholipases are activated which create holes in the cell membrane releasing cellular contents including various enzymes and metabolites. By analyzing blood serum, information regarding liver health can be

determined. Results are summarized in Table 3.5. For the 0H post-PH animals, the tests showed a significant difference between CXXC1$^{fl/fl}$ AlbCre+ and CXXC1$^{fl/fl}$ AlbCre- animals for the following parameters: cholesterol ($p \leq 0.01$), triglycerides ($p \leq 0.01$), total protein ($p \leq 0.01$), alkaline phosphatase ($p \leq 0.01$), and bilirubin total ($p \leq 0.05$). Cholesterol, triglyceride, and total protein levels were elevated in the CXXC1$^{fl/fl}$ AlbCre- animals whereas the alkaline phosphatase and bilirubin total levels were elevated in the CXXC1$^{fl/fl}$ AlbCre+ animals. For the 48H post-PH animals the following parameters differed significantly between the two groups: cholesterol ($p \leq 0.01$), triglycerides ($p \leq 0.01$), alkaline phosphatase ($p \leq 0.01$), bilirubin direct ($p \leq 0.05$), and bilirubin total ($p \leq 0.01$). Cholesterol, triglyceride, and bilirubin direct levels were elevated in the CXXC1$^{fl/fl}$ AlbCre- animals whereas alkaline phosphatase and bilirubin total levels were elevated in CXXC1$^{fl/fl}$ AlbCre+ animals. For the 5D post-PH animals the following parameters differed significantly: triglycerides ($p \leq 0.01$), total protein ($p \leq 0.01$), albumin ($p \leq 0.01$), alkaline phosphatase ($p \leq 0.01$), and ALT ($p \leq 0.01$). Triglyceride, total protein, and albumin levels were elevated in CXXC1$^{fl/fl}$ AlbCre- animals alkaline phosphatase and ALT levels were elevated in CXXC1$^{fl/fl}$ AlbCre+ animals. For the 10D post-PH animals the following parameters differed significantly between the two groups: triglycerides ($p \leq 0.05$), alkaline phosphatase ($p \leq 0.01$), AST ($p \leq 0.05$), ALT ($p \leq 0.05$), and bilirubin total ($p \leq 0.05$). Triglyceride levels were elevated in CXXC1$^{fl/fl}$ AlbCre- animals whereas alkaline phosphatase, AST, ALT, and bilirubin total levels were elevated in CXXC1$^{fl/fl}$ AlbCre+ animals.

Serum analysis of the bilirubin direct and cholesterol levels was below the instrument reading threshold for some samples. For these samples, the values were

designated as <0.1mg/dL for bilirubin direct and <25mg/dL for cholesterol. In order to analyze this data, a range was calculated for the average by using extreme values. For example for bilirubin direct, when calculating the minimum possible value of the average 0 was used as the value for the given sample. When calculating the maximum possible value of the average for bilirubin direct, 0.1 was used as the value.

To calculate statistical significance for these parameters when the average of one group was a discrete value and the other group's average was a range, the two averages were compared to determine which average was higher. If the average consisting of a range was higher then the lower end of the range was used to calculate statistical significance and vice versa, if the average consisting of a discrete value was higher then the high end of the range was used to calculate the statistical significance. To calculate statistical significance for parameters where both groups had ranges for their averages, all combinations of minimum and maximum ranges were analyzed and the least significant value was utilized.

Table 3.5. Blood Serum Parameter Values at Various Time Points Post-PH

	CXXC1fl/fl AlbCre- Mice				CXXC1fl/fl AlbCre+ Mice				
Time Point	0H	48H	5D	10D	0H	48H	5D	10D	Units
Cholesterol	84.17	57.40	70.17	66.00	17.00 - 27.00	23.60 - 28.60	27.25 - 39.75	37.25 - 43.50	mg/dL
Triglycerides	115.00	51.20	90.83	84.60	51.00	34.60	45.00	35.75	mg/dL
Total Protein	5.73	4.72	5.33	5.22	5.30	4.18	4.50	4.82	g/dL
Albumin	2.95	2.44	2.88	2.77	2.99	2.32	2.47	2.75	g/dL
Alk Phos	78.50	118.00	76.50	100.80	268.80	525.20	250.80	326.86	U/L
ALT	27.67	308.25	40.67	43.80	49.40	211.80	57.40	145.20	U/L
AST	109.33	616.40	154.00	124.80	163.40	563.60	202.40	308.20	U/L
Bilirubin, Direct	0.00 - 0.10	0.00 - 0.10	0.00 - 0.10	0.00 - 0.10	0.40 - 0.44	0.88 - 0.90	0.78 - 0.80	1.38	mg/dL
Bilirubin, Total	0.17	0.20	0.25	0.16	0.94	1.90	1.46	2.74	mg/dL

3.6 H&E Slide Histology for Post-PH Male Mice

Enlarged hepatocytes were observed throughout the various time points examined post-PH in the CXXC1$^{fl/fl}$ AlbCre+ animals. These mice at 0H often contained some of these cells, however, there was an increase in the number of these cells at later time points post-PH resulting in large patches present throughout the liver. In many of these cells, a progression of the nuclear envelope dissolving and genetic material dropping out of the cell was observed leaving discolored large patches.

At 24H post-PH, minor lipid accumulation was observed in the CXXC1$^{fl/fl}$ AlbCre+ mouse livers but not the CXXC1$^{fl/fl}$ AlbCre- mouse livers. At 36H post-PH, lipid accumulation was observed in the CXXC1$^{fl/fl}$ AlbCre- livers. In the CXXC1$^{fl/fl}$ AlbCre+ animals, there was an increase in lipid accumulation which was primarily concentrated around the enlarged hepatocytes. At 48H post-PH, the CXXC1$^{fl/fl}$ AlbCre- animals still exhibited some lipid accumulation and many mitotic figures visible. In comparison, the CXXC1$^{fl/fl}$ AlbCre+ livers had a decreased amount of mitotic figures. At 72H post-PH, mitotic figures were still visible in the CXXC1$^{fl/fl}$ AlbCre- livers but in comparison a markedly decreased amount were present in the CXXC1$^{fl/fl}$ AlbCre+ livers. In addition, there are no lipid droplets observed in the cells for either genotype by this time point. At 5D post-PH, some mitotic figures are still visible in the CXXC1$^{fl/fl}$ AlbCre- animals and some are also present in the CXXC1$^{fl/fl}$ AlbCre+ animals. At 10D post-PH, there are very few mitotic figures still visible in the CXXC1$^{fl/fl}$ AlbCre- animals and some present in the CXXC1$^{fl/fl}$ AlbCre+ animals. Figure 3.6 displays these results.

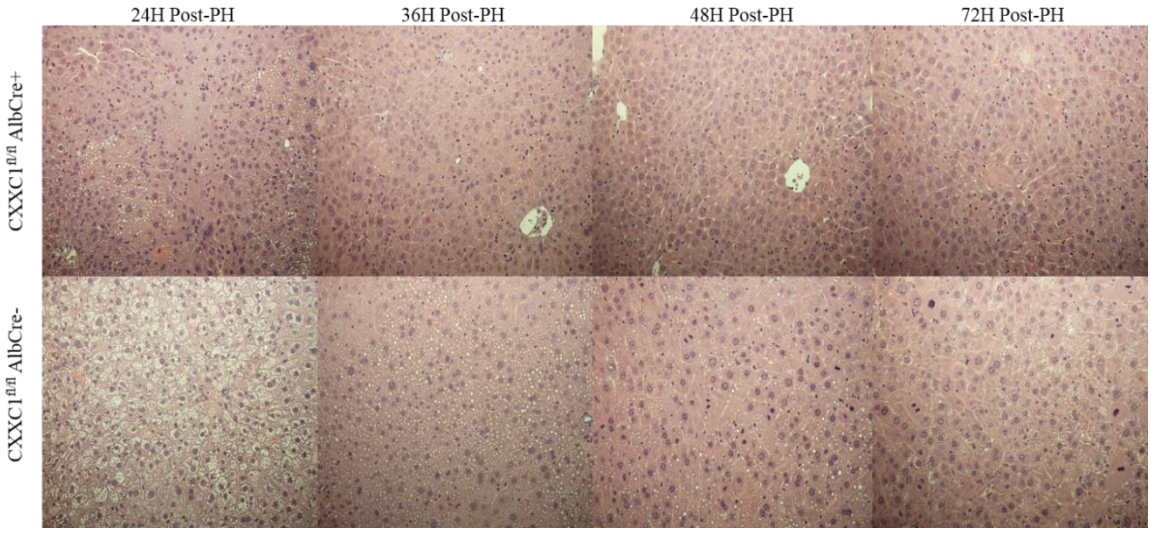

Figure 3.6. Histological Differences between CXXC1$^{fl/fl}$ AlbCre+ and CXXC1$^{fl/fl}$ AlbCre- Males at Hourly Time Points Post-PH

Male mice (n = 5, 6) between the ages of approximately 3 to 6 months were subjected to partial hepatectomies and sacrificed at various hourly time points. Their livers were harvested and preserved in 10% neutral buffered formalin until H&E staining was performed. Slides were imaged at 200x magnification and are displayed chronologically from left to right to visualize cell changes following partial hepatectomy. The top row shows the liver histology of CXXC1$^{fl/fl}$ AlbCre+ mice and the bottom row shows the histology of CXXC1$^{fl/fl}$ AlbCre- mice.

3.7 Deficiency of Hepatic CFP1 in Female Mice Caused Diminished Liver Regeneration Post-PH

The average liver:body mass ratio was calculated for both CXXC1$^{fl/fl}$ AlbCre+ females and CXXC1$^{fl/fl}$ AlbCre- females at 5 days and 10 days post-PH (Figure 3.7). The ratio was significantly different ($p \leq 0.05$) for these two genotypes at both time points. At 5 days post-PH, CXXC1$^{fl/fl}$ AlbCre+ females had a liver:body ratio of 2.91% and CXXC1$^{fl/fl}$ AlbCre- females had a liver:body ratio of 3.40%. At 10 days post-PH, CXXC1$^{fl/fl}$ AlbCre+ females had a liver:body ratio of 3.08% and CXXC1$^{fl/fl}$ AlbCre- females had a liver:body ratio of 3.63%.

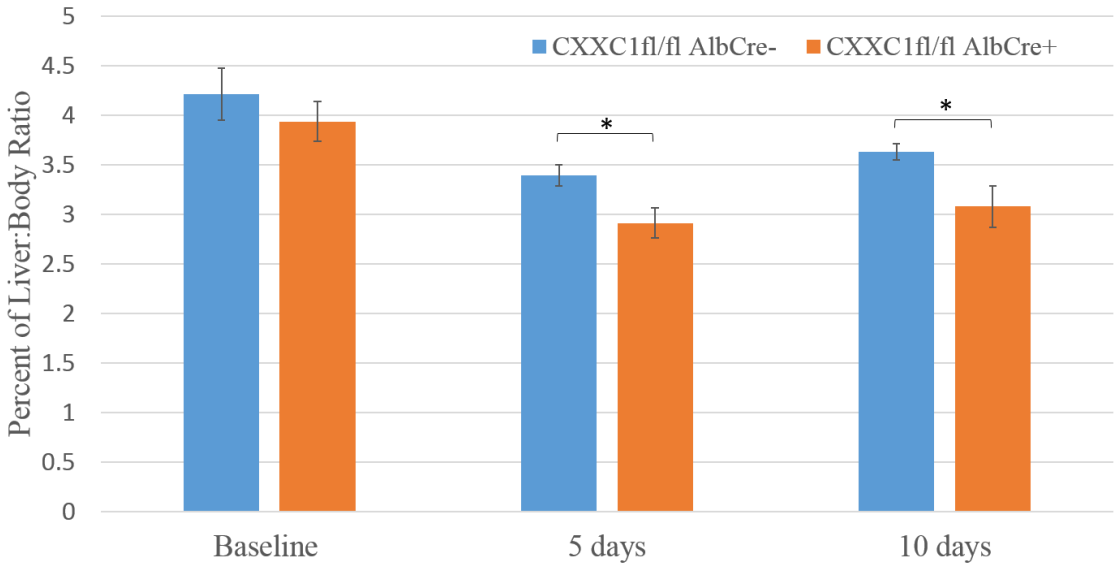

Figure 3.7. Female Liver Regeneration Hampered in CFP1-deficient Mice

Female mice (n= 5,6,7) between the age of approximately 3 to 6 months were subjected to partial hepatectomies and then sacrificed at various time points following the partial hepatectomy. The total body weight and the liver weight were measured at the time of death. The liver:body ratio was calculated based on these measurements. A graph was constructed to display the liver:body ratio percentage for both genotypes at each of the time points studied. The blue bars represents the CXXC1$^{fl/fl}$ AlbCre- mice and the orange bars represents the CXXC1$^{fl/fl}$ AlbCre+ mice. Significance is denoted by asterisks with one asterisk signifying $p<0.05$.

3.8 Mice on Fast Food Diet with CFP1-deficient Livers Experienced Decreased Weight Gain and Liver Expansion

The weight increase over the seven months on the prescribed diet was determined by calculating the difference between the pre-diet weight and the weight at time of death. This value was averaged for all individuals within a treatment group to determine the overall trend for each group (Figure 3.8). Due to higher levels of fat, fructose, and cholesterol in the fast food diet, the results showed a strong significance ($p \leq 0.01$) between the weight gained by animals on the control diet when compared to those on the fast food diet for both genotypes. Interestingly there was also a significant difference ($p \leq 0.05$) observed between the $CXXC1^{fl/fl}$ AlbCre+ and $CXXC1^{fl/fl}$ AlbCre- animals that were on the fast food diet. $CXXC1^{fl/fl}$ AlbCre+ animals on the fast food diet average gained 16.69 grams over the seven months compared to the 24.58 grams gained by the $CXXC1^{fl/fl}$ AlbCre- on average.

The liver:body ratio was calculated in the aforementioned manner and averaged for each treatment group. (Figure 3.8). $CXXC1^{fl/fl}$ AlbCre- animals on the fast food diet had an average liver:body ratio of 7.45% whereas those on the control diet had an average liver:body ratio of 5.37%. $CXXC1^{fl/fl}$ AlbCre+ animals on the fast food diet had an average liver:body ratio of 4.98% and those on the control diet had an average liver:body ratio of 4.38%. Statistical analysis showed a significant difference ($p \leq 0.01$) when comparing individuals on the same diet but with different genotypes. There was also a significant difference ($p \leq 0.01$) between the $CXXC1^{fl/fl}$ AlbCre- animals on the fast food diet and those on the control diet. Interestingly this trend did not apply to the $CXXC1^{fl/fl}$ AlbCre+ animals. Despite experiencing an increase in overall body weight

due to the diet, these animals were not able to undergo the liver expansion seen in the $CXXC1^{fl/fl}$ AlbCre- animals.

Figure 3.8. Differences in Weight Gain and Liver Expansion as a Result of Diet and CFP1-deficiency

A. Male mice between the age of approximately 3 to 6 months were individually housed and fed either the fast food diet (n = 9, 10) or control diet (n = 3) for 7 months. Mice were weighed weekly. The weight gain over the 7 months was calculated by subtracting the initial weight from the weight at time of death. The weight gain was graphed in order to visualize differences resulting from diet and genotype. Asterisks denoted significance with one asterisk signifying $p<0.05$ and two signifying $p<0.01$.

B. Male mice between the age of approximately 3 to 6 months were individually housed and fed either a fast food diet (n = 9, 10) or control diet (n = 3). Following 7 months on their assigned diet, the mice were sacrificed and their total body weight and liver mass were measured. The liver:body weight ratio was calculated and this data was graphed in order to visualize differences in liver expansion as a result of diet. Asterisks denoted significance with two asterisks signifying $p<0.01$.

A

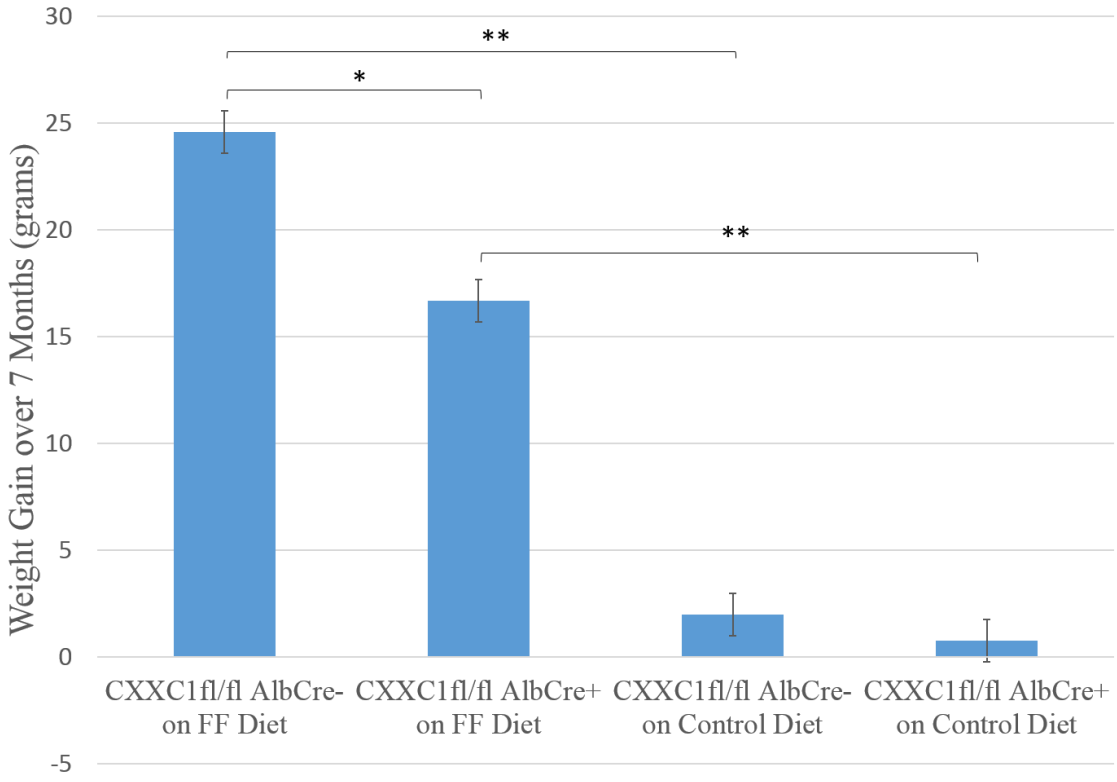
Weight Gain over 7 Months (grams)
30
25
20
15
10
5
0
-5
**
*
**
CXXC1fl/fl AlbCre- on FF Diet
CXXC1fl/fl AlbCre+ on FF Diet
CXXC1fl/fl AlbCre- on Control Diet
CXXC1fl/fl AlbCre+ on Control Diet

B

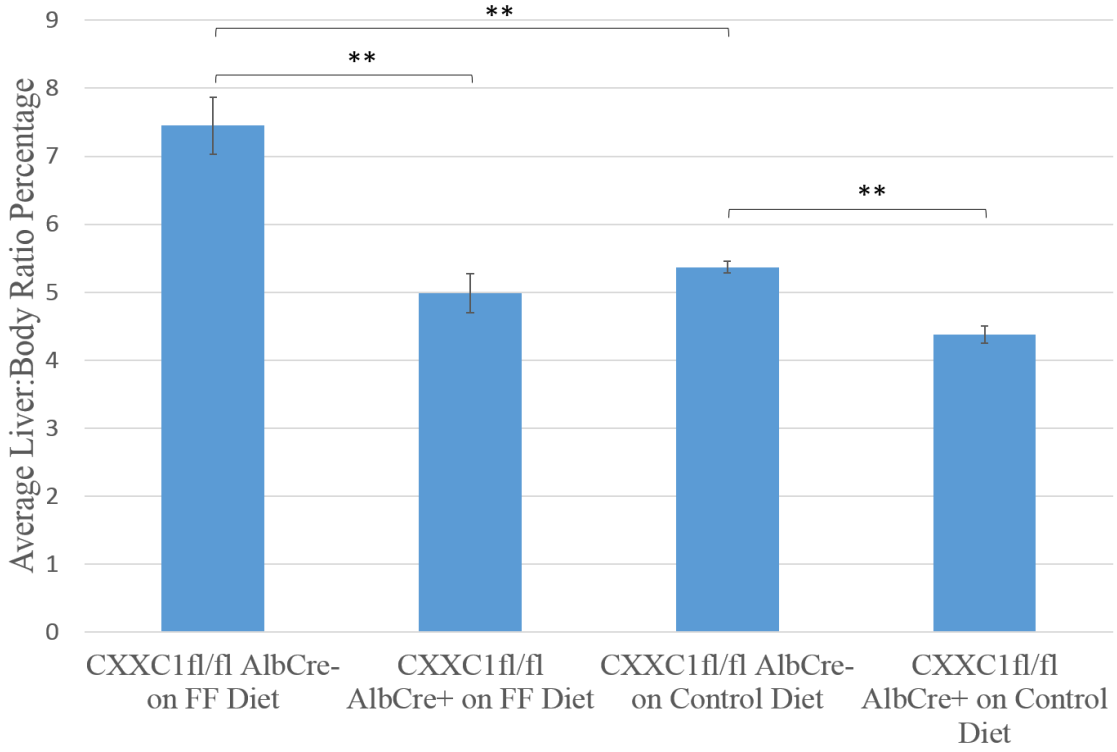
Average Liver:Body Ratio Percentage
9
8
7
6
5
4
3
2
1
0
**
**
**
CXXC1fl/fl AlbCre- on FF Diet
CXXC1fl/fl AlbCre+ on FF Diet
CXXC1fl/fl AlbCre- on Control Diet
CXXC1fl/fl AlbCre+ on Control Diet

3.9 Blood Serum Analysis for NASH Model Animals

The results from the blood serum analysis demonstrated a significant difference for the following parameters between the CXXC1$^{fl/fl}$ AlbCre+ and CXXC1$^{fl/fl}$ AlbCre- animals that were on the fast food diet for seven months: cholesterol ($p \leq 0.01$), triglycerides ($p \leq 0.05$), ALT ($p \leq 0.01$), AST ($p \leq 0.05$), and bilirubin direct ($p \leq 0.05$). Cholesterol, ALT, AST, and bilirubin direct levels were higher in the CXXC1$^{fl/fl}$ AlbCre- animals while the triglyceride level was higher in CXXC1$^{fl/fl}$ AlbCre+ animals. The CXXC1$^{fl/fl}$ AlbCre+ mice on the control diet for seven months had significantly different values for the following serum parameters in comparison to the CXXC1$^{fl/fl}$ AlbCre- mice on the control diet: cholesterol ($p \leq 0.01$) and triglycerides ($p \leq 0.05$). Both of these values were elevated in the CXXC1$^{fl/fl}$ AlbCre- animals.

Comparison of CXXC1$^{fl/fl}$ AlbCre- animals on the fast food diet with animals of the same genotype on the control diet showed significant differences in the following parameters: cholesterol ($p \leq 0.01$), total protein ($p \leq 0.01$), alkaline phosphatase (($p \leq 0.05$), and ALT (($p \leq 0.01$). Cholesterol, total protein, alkaline phosphatase, and ALT levels were elevated in the CXXC1$^{fl/fl}$ AlbCre- animals on the fast food diet. Comparison of the CXXC1$^{fl/fl}$ AlbCre+ animals on the fast food diet with animals of the same genotype on the control diet showed significant differences in the following serum parameters: cholesterol, triglyceride, total protein, and albumin. Cholesterol, triglyceride, total protein and albumin levels were elevated in the CXXC1$^{fl/fl}$ AlbCre+ animals on the fast food diet.

Serum analysis of bilirubin direct was below the instrument reading threshold for some samples. For these samples, the values were designated as <0.1mg/dL for bilirubin direct. The serum analysis for these samples was performed in the same manner as with

the post-PH samples. All of the serum parameter values for the four groups are summarized in Table 3.9.

Table 3.9. Blood Serum Paramters After 7 Months on Respective Diets

	CXXC1fl/fl AlbCre- Mice on Fast Food Diet	CXXC1fl/fl AlbCre+ Mice on Fast Food Diet	CXXC1fl/fl AlbCre- Mice on Control Diet	CXXC1fl/fl AlbCre+ Mice on Control Diet	
Cholesterol	294.33	170.25	85.00	34.33	mg/dL
Triglycerides	106.67	145.13	127.33	66.00	mg/dL
Total Protein	6.40	6.14	5.83	5.60	g/dL
Albumin	3.18	3.26	3.07	2.93	g/dL
Alk Phos	181.44	159.75	116.67	182.33	U/L
ALT	320.78	119.38	61.67	71.67	U/L
AST	592.00	383.63	739.33	402.00	U/L
Bilirubin, Direct	0.03 - 0.10	0.01 - 0.03	0.00 - 0.10	0.13 - 0.20	mg/dL
Bilirubin, Total	0.37	0.31	0.20	0.57	mg/dL

3.10 Liver Histology of NASH Mice

H&E analysis of the livers of mice on the fast food diet when compared to the livers of mice on the control diet showed a marked increase in lipid accumulation. The distribution of the lipid accumulation as well as the size of the hepatocytes differed between the CXXC1$^{fl/fl}$ AlbCre+ and CXXC1$^{fl/fl}$ AlbCre- animals. The CXXC1$^{fl/fl}$ AlbCre- livers display severe steatosis with both microvesicular and macrovesicular steatosis present throughout the tissue. CXXC1$^{fl/fl}$ AlbCre+ animals displayed significantly reduced lipid accumulation with minor macrovesicular steatosis. There may have also been microvesicular steatosis, however, it is possible that it was cellular ballooning. In addition, the livers of the CXXC1$^{fl/fl}$ AlbCre+ animals displayed a patchy appearance in comparison to the CXXC1$^{fl/fl}$ AlbCre- mice (Figure 3.10).

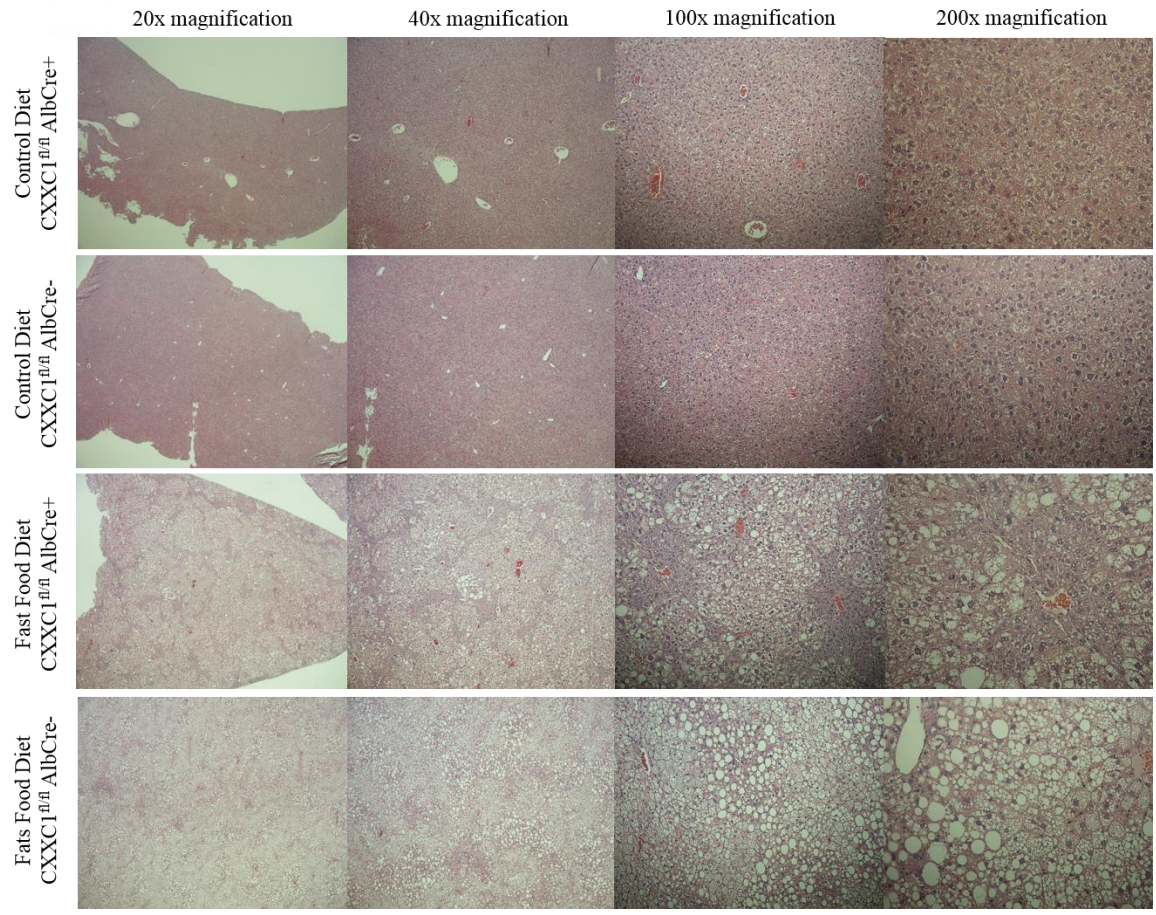

Figure 3.10. CFP1-deficiency Results in Altered Lipid Accumulation

Male mice between the ages of approximately 3 to 6 months were individually housed and fed either a fast food diet (n = 9, 10) or control diet (n =3). Following 7 months on their assigned diet, the mice were sacrificed. Their livers were harvested and preserved in 10% neutral buffered formalin until H&E staining was performed. Slides were imaged at 20x, 40x, 100x, and 200x magnification to visualize cellular changes as a result of the diets and CFP1-deficiency. The top two rows depict mice on the control diet and the bottom two rows depict mice on the fast food diet.

CHAPTER 4. DISCUSSION

4.1 Hepatic CFP1-deficiency in Unperturbed Liver

Under normal conditions, it was shown that the hepatic CFP1-deficiency in male mice resulted in smaller liver:body ratios. However, this was not the case in the female mice. For females, there was no significant difference between the CXXC1$^{fl/fl}$ AlbCre+ females and CXXC1$^{fl/fl}$ AlbCre- females in terms of liver:body ratio. Despite this, the histology of the females showed more of the enlarged hepatocytes characteristic of the CFP1-deficient livers than seen in the male mice indicating that the females were also experiencing liver damage. These results suggest the presence of hepatic sexual dimorphism.

The occurrence of sexual dimorphism in regards to CFP1-deficiency is unsurprising. It is widely accepted that under normal conditions liver sexual dimorphism exists. Proteins called the regulators of sex-limitation (RSL1 and RSL2) have been discovered which belong to the family of Krüppel-associated box zinc finger proteins (KRAB-ZFPs). These KRAB-ZFPs serve as epigenetic regulators of liver-associated genes and restrict DNA to its heterochromatin state. In pre-puberty mice, RSL1 and RSL2 have been found to repress male-specific hepatic genes in both males and females. During puberty, pulsatile GH signaling in males causes alleviation of the repression allowing for adult sexual dimorphism of the liver. A limited number of RSL gene targets are known, such as Slp, Cyp2d9, and Mup. In addition to the RSL proteins, STAT5b has been identified as a gene important for hepatic sexual dimorphism.[30, 56] Some of the effects of the sexual dimorphism are body mass and steroid and drug metabolism

differences. It is possible that differences in hepatic gene expression result in CFP1-deficiency having differing effects dependent on mouse sex.

4.2 CFP1-deficiency in the Maternal Liver

Pregnancy-induced hepatomegaly is a necessary physiological event that occurs in response to the increased metabolic demands placed on the murine maternal liver by fetuses. It is accompanied by changes in gene expression, including genes involved in cell proliferation, cytokine signaling, liver regeneration, and metabolism.[50] Previous observations suggested that CXXC1$^{fl/fl}$ AlbCre+ females were unable to conceive pups. This led to concerns that the absence of CFP1 in the liver prevented the changes in gene expression necessary for pregnancy-induced hepatomegaly. This study confirmed these observations in CXXC1$^{fl/fl}$ AlbCre+ females mated with CXC1$^{fl/fl}$ AlbCre- males. It showed that despite being able to bring mouse pups to term, the CXXC1$^{fl/fl}$ AlbCre+ females mated with CXXC1$^{fl/fl}$ AlbCre- males experienced difficulties during parturition with over half of them undergoing dystocia. It has been demonstrated in dystotic female cows through blood serum analysis that uterine torsion is associated with hepatocellular damage thus supporting the assertion that there is a link between these cases of dystocia and the liver dysfunction present in these females.[26]

Interestingly females with the same genotype that were mated with C57 BL/6 males and CXXC1$^{fl/wt}$ AlbCre- males did not experience this increased risk of dystocia. These observations may have been the result of small sample sizes of CXXC1$^{fl/fl}$ AlbCre+ females mated with genotypes other than CXXC1$^{fl/fl}$ AlbCre- males. If the observed differences in pregnancy success based on male genotype are replicated with further matings this would imply that the prenatal environment is not the only pertinent

factor. The genotype of the pups may be another factor resulting in the observed proclivity for dystocia. The pup genotype may result in fetomaternal disproportion causing difficulties during parturition. A manifestation of fetomaternal disproportion could be if the pups were large and the dam's pelvis was small resulting in the pups becoming lodged in the birthing canal and subsequently dystocia.

It would be beneficial to set up more breeding cages of $CXXC1^{fl/fl}$ AlbCre+ females mated with C57 BL/6 males and $CXXC1^{fl/wt}$ AlbCre- males to determine if these breedings also result in dystocia. The most significant waves of hepatocyte proliferation in maternal livers occur at 8, 13, and 15 days post-coitus and as such these are days of interest to examine differences in liver:body ratios between CFP1-deficient livers and CFP1-expressing livers as well as changes in gene profiles.[19] Another possible direction could be to determine if due to the proposed lack of maternal liver expansion in the CFP1-deficient animals there is a decreased level of fitness for the pups. Possible means of examining this include decreased litter size and decreased total body mass at birth and following birth compared to age matched pups from mothers containing the CFP1 gene.

4.3 Role of CFP1 in Regenerating Liver

Liver regeneration post-PH necessitates changes in gene expression patterns in order for quiescent hepatocytes to re-enter the cell cycle. The promoters of most cell-cycle promoters have unmethylated CpGs and H3K4me marks making these genes transcriptionally active. Due to CFP1's role in establishing methylation patterns and therefore determining whether or not genes are transcriptionally active, it was anticipated that in CFP1-deficient livers hepatocytes would not be able to replicate to regenerate the lost mass. The results supported this hypothesis by demonstrating a significantly reduced

capacity for regeneration in the CXXC1$^{fl/fl}$ AlbCre+ males starting at 48H post-PH. The difference between male CXXC1$^{fl/fl}$ AlbCre+ and the CXXC1$^{fl/fl}$ AlbCre- males continued to increase at later time points as the CXXC1$^{fl/fl}$ AlbCre- males regained their mass while regeneration occurred at a much slower rate in the male CXXC1$^{fl/fl}$ AlbCre+.

The H&E results provided more insight into what was occurring in the hepatocytes to cause differences in regenerative capacity. At 0H post-PH, the liver:body ratio of CXXC1$^{fl/fl}$ AlbCre+ males did not differ significantly when compared to CXXC1$^{fl/fl}$ AlbCre- males. At 24H post-PH, lipid accumulation began in the CXXC1$^{fl/fl}$ AlbCre+ livers. This continued on into the 36H post-PH and 48H post-PH in the livers of individuals with both genotypes. In the male CXXC1$^{fl/fl}$ AlbCre+ mouse livers, the lipid accumulation was found primarily in the enlarged hepatocytes starting at 36 and 48 hours post-PH. This lipid accumulation has been documented under normal conditions between 24 to 48 hours post-PH as a means for cells to acquire the energy necessary for replication as well as to create a lipid bilayer for the daughter cell. Therefore at this point both the CXXC1$^{fl/fl}$ AlbCre+ and CXXC1$^{fl/fl}$ AlbCre- male livers were preparing themselves for mitosis.

48H post-PH was the time point at which the liver:body mass ratio of the two genotypes initially became significantly different. This coincided with a larger number of male CXXC1$^{fl/fl}$ AlbCre- hepatocytes undergoing mitosis than male CXXC1$^{fl/fl}$ AlbCre+ hepatocytes. Hence it appears that the absence of CFP1 leads to inability of cells to transition to mitosis. During mitosis, the centromere is important as the site of chromosomal segregation. The centromere is transcriptionally active and necessitates a balance of euchromatin and heterochromatin to function. Bergmann, *et al.*, showed by

utilizing a non-essential human artificial chromosome that depletion of H3K4me2 marks results in mitotic instability, severely decreased levels of centromeric proteins CEN-A and CEN-P, and α-satellite transcription.[50] The absence of CFP1 could result in inappropriate H3K4me2 marks and therefore result in the mitotic problems Bergmann observed.

By 5 and 10 days post-PH the male CXXC1$^{fl/fl}$ AlbCre- livers had successfully regenerated their mass resulting in a larger difference between the two groups. The level of significance was a little lower for the 10 days post-PH animals. Therefore it may be that the CXXC1$^{fl/fl}$ AlbCre+ males are able to gradually regenerate their liver but it is occurring at a much reduced rate. It may be worthwhile to set up another time point at 15 days post-PH to see if given more time they are able to recover the lost liver mass.

A limited amount of post-PH data was collected and analyzed for the female mice. The collected data indicated that similar to male CXXC1$^{fl/fl}$ AlbCre+ mice, female CXXC1$^{fl/fl}$ AlbCre+ mice experienced delayed generation compared to CFP1-expressing counterparts. It would be beneficial to create a 0H time point for the female mice as was done with the males in order to better visualize the rate of regeneration. It would be of interest to look at the same hourly time points post-PH examined in the males as well as the 15 days post-PH for the females in order to assess any sex-differences in rate of regeneration.

4.4 Enlarged Hepatocytes Observed in Histology

The observed enlarged hepatocytes were an intriguing, consistent indicator as to the genotype of a liver. These enlarged cells were only observed in the CXXC1$^{fl/fl}$ AlbCre+ animals and were found in patches. At 0H post-PH there were a nominal

amount of these enlarged hepatocytes. The location of the lipid accumulation witnessed starting at 24H post-PH in the CXXC1$^{fl/fl}$ AlbCre+ livers suggests that the enlarged cells were the cells attempting to prepare for mitosis. In some of these cells it was possible to observe the nuclear envelope dissolving which occurs during prophase. The cells were observed to not only halt mid-cell cycle but also undergo some type of cell death.

Typically hepatic cell death occurs either by apoptosis or necrosis.[24] It is likely that under these circumstances due mitosis being unable to proceed, the cell reacts by initiating self-destruction. It would be expected that if the cell is responding to internal signals then apoptosis would be the mode of cell death occurring, however, it is possible that a combination of the two modes is occurring. It would be possible to look for apoptotic cells by performing a TUNEL assay or IHC staining for caspase 3 or p53. Necrotic cells could be identified by staining for cyclophylin A.[15]

4.5 Gallbladder Phenotype in Livers Subjected to Partial Hepatectomies

The gallbladder serves as the storage site of bile acids produced by hepatocytes. These bile acids play important roles in the body by breaking down fats and clearing the liver of contaminants. Based on their role in breaking down and storing fats, the enlarged gallbladders seen in the fast food animals are unsurprising, however, this is not the case for the mice with CFP1-deficient livers used in the partial hepatectomy study. In humans, alkaline phosphatase levels three or more times elevated in comparison to control levels can suggest obstructions in the common bile duct or the intrahepatic bile ducts.[8] These high levels of alakaline phosphatase were observed in all of the CXXC1$^{fl/fl}$ AlbCre+ mice when compared to their controls. Therefore perhaps due to an obstruction in bile flow, bile builds up in the gallbladder causing the observed phenotype.

Interestingly, bile acids have also been found to play a role in liver regeneration with elevated levels corresponding with accelerated regeneration while decreased levels have been correlated with decreased regeneration.[25] Therefore it is possible that the regenerative ability of CFP1 mice is further hampered by the diminished bile flow. In response, the hepatocytes may attempt to produce more bile but due to the severely reduced hepatocyte count the gallbladder size does not begin to increase in response to bile production until a period of time has passed during which hepatocyte number can increase. A more consistent means of scoring gallbladder size must be developed in order to further elucidate the difference seen between animals with normal and CFP1-deficient livers and to generate a timeline. It may also be of interest to examine bile acid levels present in blood serum to determine if a difference is present between the two genotypes examined.

4.6 Differences in Blood Serum Composition in Post-PH Animals

The parameters examined by the blood serum analysis indicate decreased metabolic function in CXXC1$^{fl/fl}$ AlbCre+ males when compared with the CXXC1$^{fl/fl}$ AlbCre- males. The reduced triglyceride levels at all time points in the CXXC1$^{fl/fl}$ AlbCre+ males indicate decreased lipogenic ability of the liver. Elevated direct bilirubin levels at all time points in the CXXC1$^{fl/fl}$ AlbCre+ males is indicative of an inability of the liver to secrete the conjugated bilirubin. This indicates the possibility of a hepatobiliary disease and is supported by the enlarged gallbladder observations as well as the elevated alkaline phosphatase levels measured in these animals.

Other measured parameters exhibit increasingly divergent values at later time points post-PH supporting the statement that CXXC1$^{fl/fl}$ AlbCre+ males experience a

decreased and potentially delayed regenerative response. This regenerative response results in greater liver injury and damage when compared with time point matched CXXC1$^{fl/fl}$ AlbCre- males. The highest levels of injury and damage were observed at the 5 and 10 day time points. The blood serum analysis showed that at 0H post-PH, the livers of the CXXC1$^{fl/fl}$ AlbCre+ males were not experiencing significant liver damage. At 48 hours, the point at which the rate of regeneration diverged for the two groups there was still no significant difference in the amount of liver injury experienced as measured by AST and ALT levels.

By the 5 day time point, significant liver damage was indicated by the significantly elevated ALT level and elevated AST level in the CXXC1$^{fl/fl}$ AlbCre+ males. In addition, these mice had significantly elevated total protein levels indicating decreased liver protein metabolism and significantly decreased albumin production. By the 10 day time point both the ALT and AST levels were significantly elevated in the CXXC1$^{fl/fl}$ AlbCre+ males. However, the albumin and total protein levels were no longer significantly different between the CXXC1$^{fl/fl}$ AlbCre+ and CXXC1$^{fl/fl}$ AlbCre- males. This suggests that delayed regeneration has occurred giving further motivation for creation of a 15D post-PH time point.

4.7 Role of CFP1 in NASH Progression

As expected due to the composition of the diets, the consumption of the fast food diet resulted in significant increases in body weight when compared to individuals of the same genotype consuming the control diet. However, the amount of weight gained differed significantly between the two groups with the CXXC1$^{fl/fl}$ AlbCre+ mice gaining less weight. One possibility is that this occurred because the CXXC1$^{fl/fl}$ AlbCre+ mice

were not consuming as much of the fast food diet and therefore were not gaining as much weight as the CXXC1$^{fl/fl}$ AlbCre- mice. This could also explain the differences seen in the liver:body weight ratios and histology results. Efforts were made to visually determine if the CXXC1$^{fl/fl}$ AlbCre+ and CXXC1$^{fl/fl}$ AlbCre- mice were consuming the same amount of food. Despite appearing to have similar consumption rates, the use of an electronic sensor to generate quantitative evidence regarding the feeding behavior of the mice would provide conclusive evidence.

The most compelling explanation for the weight gain and hepatomegaly observed in the CXXC1$^{fl/fl}$ AlbCre- mice is the onset of insulin resistance (IR) which is highly correlated with NASH. IR can be induced by overeating and obesity. The high levels of free fatty acids from the fast food diet combined with reduced suppression of lipolysis due to IR would have resulted in increased fatty infiltration of the liver. It would be of interest to analyze blood-insulin levels to confirm this hypothesis through either a euglycemic clamp or glucose tolerance test. If no difference between the food consumption of the CXXC1$^{fl/fl}$ AlbCre+ mice and CXXC1$^{fl/fl}$ AlbCre- mice exists and IR is the cause of the weight gain and hepatomegaly then it is possible that hepatic CFP1-deficiency prevents the development of IR and diabetes or diminishes its effects on the liver.

To explain the effects seen in the CXXC1$^{fl/fl}$ AlbCre+ mice, the effects of the fast food diet must be considered. The diet results in increased fat accumulation in the body which corresponds with increased total body lipolysis. This results in increased levels of free fatty acids which the liver then uptakes. Therefore, if transport of the lipids to the liver is prevented this would inhibit hepatic lipid accumulation. This has been

demonstrated in mice that lack the primary fatty acid transporter, fatty acid transporter 5 (FATP5). These mice show resistance to diet-induced steatohepatitis.[45] It is possible that CFP1-deficiency is causing repression of FATP5 and resulting in decreased fat accumulation in the liver consistent with both the histology results and liver:body mass measurements. Despite this explaining the difference in liver size, this would not explain the significant difference in weight gain between the $CXXC1^{fl/fl}$ AlbCre+ mice and $CXXC1^{fl/fl}$ AlbCre- mice.

It is possible that another factor is causing the body mass differences. Interestingly, the RSL1 gene associated with sexual dimorphism may contribute to the differences seen between the $CXXC1^{fl/fl}$ AlbCre+ mice and $CXXC1^{fl/fl}$ AlbCre- mice. Male mice expressing RSL1 only in the liver on a high fat diet gained approximately half the weight gained by wild-type or RSL1-deficient male mice on a high fat diet. These mice demonstrated both decreased diet-induced weight gain as well as suppressed lipogeneic genes in white adipose tissue demonstrating RSL1's role in liver to adipose communication.[30] Therefore altered RSL1 may contribute to the differences in weight gain between the $CXXC1^{fl/fl}$ AlbCre+ mice and $CXXC1^{fl/fl}$ AlbCre- mice.

4.8 Altered Hepatic Lipid Accumulation in NASH Animal Models with CFP1-deficient Livers

Liver histology showed that consumption of the fast food diet resulted in increased lipid accumulation compared to individuals consuming the control diet. The histology also showed striking differences in lipid accumulation in the liver between the $CXXC1^{fl/fl}$ AlbCre+ and $CXXC1^{fl/fl}$ AlbCre- mice on the fast food diet including differences in macrovesicular and microvesicular steatosis. Macrovesicular steatosis is

considered the more benign form whereas microvesicular often has more serious connotations. In the liver, fat initially accumulates in vacuoles which coalesce into macrovesicular lipid droplets. Therefore macrovesicular steatosis is associated with continuous elevated triglyceride levels. Microvesicular steatosis occurs under conditions of metabolic disruption.

The presence of both forms of steatosis in the CXXC1$^{fl/fl}$ AlbCre- mice suggests severe liver disease. The CXXC1$^{fl/fl}$ AlbCre+ mice liver histology is inconclusive due to the need to differentiate between microvesicular steatosis and cellular ballooning. Regardless, it does appear that the CXXC1$^{fl/fl}$ AlbCre+ mice are experiencing a degree of hepatic stress although it appears to be diminished in comparison to the CXXC1$^{fl/fl}$ AlbCre- mice on the fast food diet. In order to better visualize the difference between microvesicular and macrovesicual steatosis, Oil Red O staining should be performed. This will also allow for accurate differentiation between microvesicular steatosis and cellular ballooning. Trichrome staining should also be performed in order to visualize fibrosis which is a key characteristic of NASH.

4.9 Differing Effects of Fast Food Diet on Blood Serum Composition Due to Different Genotypes

Under the control diet condition, the cholesterol and triglyceride levels differed significantly between the CXXC1$^{fl/fl}$ AlbCre+ and CXXC1$^{fl/fl}$ AlbCre- mice indicating differences in metabolism. The significantly decreased levels of triglycerides were also observed in the CXXC1$^{fl/fl}$ AlbCre+ mice at the 0H post-PH time point. These animals ranged between 3 to 5 months old whereas the animals for the diet study ranged from 8 to

9 months. Therefore as animals age, the deficiency of CFP1 may result in altered cholesterol metabolism.

The $CXXC1^{fl/fl}$ AlbCre- animals on the fast food diet had elevated levels of cholesterol compared to individuals of the same genotype on the control diet. This is most likely due to differences in diet composition. The fast food diet contained 20,000 ppm cholesterol whereas the control diet contained 209 ppm cholesterol. Elevation of total protein levels, ALT levels, and AST levels is indicative of liver injury which is consistent with the progression of NASH and IR in these animals as a result of their diet. There was also an insignificant decrease in the level of triglycerides in the animals on the fast food diet which may be due to IR.

The triglyceride and cholesterol levels were significantly elevated in the $CXXC1^{fl/fl}$ AlbCre+ animals on the fast food diet which is likely due to the composition of the diet. Albumin levels were significantly elevated possibly due to its role in transporting fatty acids and the high fatty acid levels resulting from the diet. Total protein levels were also significantly elevated. This may have been the result of the elevated albumin levels because albumin constitutes approximately half of serum protein.

Comparison of the $CXXC1^{fl/fl}$ AlbCre+ and $CXXC1^{fl/fl}$ AlbCre- animals on the fast food diet revealed a higher degree of liver injury and decreased liver function in the $CXXC1^{fl/fl}$ AlbCre- animals. The cholesterol levels were elevated in the $CXXC1^{fl/fl}$ AlbCre- animals and the triglyceride levels were reduced suggesting decreased lipogenic ability of the liver. Significantly elevated ALT and AST values provided further evidence for liver damage in the $CXXC1^{fl/fl}$ AlbCre- animals. As noted prior, differences in fast food diet consumption may have factored into these results. If consumption rates did not

differ then collectively the data suggests that CFP1-deficiency confers resistance to the effects of diet-induced NASH in mouse livers.

4.10 Future Directions

This study was successful in demonstrating that CFP1 is a critical epigenetic regulator for maintaining liver homeostasis under the three scenarios studied: pregnancy induced hepatomegaly, liver regeneration, and NASH progression. It also successfully demonstrated sex-differences in the role of CFP1 under unperturbed and delayed post-PH time points. It would be of interest to examine the effects of CFP1-deficiency at additional time points post-PH in the female in order to generate a more complete picture of female liver regeneration as well as on the fast food diet to examine the female progression of NASH.

Future work should examine the gene targets of CFP1 and the disruption of normal gene transcription patterns as a result of CFP1-deficiency. In order to examine this, various procedures need to be performed including, Western Blots to look for H3K4me3 marks, ELISA to measure genomic levels of 5-methylcytosine, CHIP-Seq to examine CFP1-DNA interactions, and RNA-Seq to analyze changes in RNA levels. These tests will provide crucial information to further elucidate the molecular basis behind CFP1's role in the liver to benefit the treatment of liver diseases.

REFERENCES

[1] Allis, C. David, and Thomas Jenuwein. "The molecular hallmarks of epigenetic control." Nature Reviews Genetics 17.8 (2016): 487-500. Web.

[2] Alva, Vikram, Moritz Ammelburg, Johannes Söding, and Andrei N. Lupas. "On the origin of the histone fold." BMC Structural Biology 7.1 (2007): 17. Web.

[3] Annunziato, Anthony T. "DNA Packaging: Nucleosomes and Chromatin." Nature Education 1(1):26 (2008).Web.

[4] Apte, Udayan. Liver regeneration: basic mechanisms, relevant models and clinical applications. Amsterdam: Elsevier/Academic Press, 2015. Print.

[5] Bannister, Andrew J, and Tony Kouzarides. "Regulation of Chromatin by Histone Modifications." Cell Research 21.3 (2011): 381–395. PMC. Web.

[6] Baratta, Janie L. et al. "Cellular Organization of Normal Mouse Liver: A Histological, Quantitative Immunocytochemical, and Fine Structural Analysis." Histochemistry and cell biology 131.6 (2009): 713–726. PMC. Web.

[7] Bellentani, Stefano. "The epidemiology of non-alcoholic fatty liver disease." Liver International 37 (2017): 81-84. Web.

[8] Berk, Paul D., and Kevin M. Korenblat. "Approach to the Patient with Jaundice or Abnormal Liver Tests." Goldman-Cecil Medicine. 25th ed. N.p.: n.p., n.d. 983-93. ClinicalKey. Web.

[9] Bestor, T.H. (2000). The DNA methyltransferases of mammals. Hum. Mol. Genet. 9, 2395-2402.Web.

[10] Bhushan, Bharat et al. "Role of Bile Acids in Liver Injury and Regeneration Following Acetaminophen Overdose." The American Journal of Pathology 183.5 (2013): 1518–1526. PMC. Web.

[11] Bowman, Gregory D., and Michael G. Poirier. "Post-Translational Modifications of Histones That Influence Nucleosome Dynamics." Chemical Reviews 115.6 (2015): 2274-295. Web.

[12] Butler, Jill S. et al. "DNA Methyltransferase Protein Synthesis Is Reduced in CXXC Finger Protein 1–Deficient Embryonic Stem Cells." DNA and Cell Biology 28.5 (2009): 223–231. PMC. Web.

[13] Charlton, M., A. Krishnan, K. Viker, S. Sanderson, S. Cazanave, A. Mcconico, H. Masuoko, and G. Gores. "Fast food diet mouse: novel small animal model of NASH with ballooning, progressive fibrosis, and high physiological fidelity to the human condition." AJP: Gastrointestinal and Liver Physiology 301.5 (2011): n. pag. Web.

[14] Chatila, Rajaa, and Brian A. West. "Hepatomegaly and Abnormal Liver Tests Due to Glycogenosis in Adults with Diabetes." Medicine 75.6 (1996): 327-33. Web.

[15] Christofferson, Dana E., and Junying Yuan. “Cyclophilin A Release as a Biomarker of Necrotic Cell Death.” Cell death and differentiation 17.12 (2010): 1942–1943. PMC. Web.

[16] Chun, Kristin T., Binghui Li, Erika Dobrota, Courtney Tate, Jeong-Heon Lee, Shehnaz Khan, Laura Haneline, Harm Hogenesch, and David G. Skalnik. "The Epigenetic Regulator CXXC Finger Protein 1 is Essential for Murine Hematopoiesis." PLoS ONE 9.12 (2014): n. pag. Web.

[17] Clouaire, Thomas et al. “Cfp1 Integrates Both CpG Content and Gene Activity for Accurate H3K4me3 Deposition in Embryonic Stem Cells.” Genes & Development 26.15 (2012): 1714–1728. PMC. Web.

[18] Clouaire, Thomas, Shaun Webb, and Adrian Bird. “Cfp1 Is Required for Gene Expression-Dependent H3K4 Trimethylation and H3K9 Acetylation in Embryonic Stem Cells.” Genome Biology 15.9 (2014): 451. PMC. Web.

[19] Dai, Guoli et al. “Maternal Hepatic Growth Response to Pregnancy in the Mouse.” Experimental biology and medicine (Maywood, N.J.) 236.11 (2011): 1322–1332. PMC. Web.

[20] Dixon, John B., Prithi S. Bhathal, and Paul E. Obrien. "Nonalcoholic Fatty Liver Disease: Predictors of Nonalcoholic Steatohepatitis and Liver Fibrosis in the Severely Obese." Gastroenterology 121.1 (2001): 91-100. Web.

[21] Fausto, Nelson. "Liver regeneration and repair: Hepatocytes, progenitor cells, and stem cells." Hepatology 39.6 (2004): 1477-487. Web.

[22] Goldberg, Aaron D., C. David Allis, and Emily Bernstein. "Epigenetics: A Landscape Takes Shape." Cell 128.4 (2007): 635-38. Web.

[23] Grompe M. "The Role of Bone Marrow Stem Cells in Liver Regeneration." Seminars in Liver Disease 23, no. 4 (2003): 363-72.

[24] Guicciardi, Maria Eugenia et al. “Apoptosis and Necrosis in the Liver.” Comprehensive Physiology 3.2 (2013): 10.1002/cphy.c120020. PMC. Web.

[25] Hollister, Anne, Patricia Okubara, J.gary Watson, and Sterling Chaykin. "Reproduction in mice: Liver enlargement in mice during pregnancy and lactation." Life Sciences 40.1 (1987): 11-18. Web.

[26] Huang, W. "Nuclear Receptor-Dependent Bile Acid Signaling Is Required for Normal Liver Regeneration." Science 312.5771 (2006): 233-36. Web.

[27] Hussein, H., and M.r. Abd Ellah. "Effects of dystocia, fetotomy and caesarian sections on the liver enzymes activities and concentrations of some serum biochemical parameters in dairy cattle." Animal Reproduction Science 105.3-4 (2008): 384-91. Web.

[28] Jin, Bilian, and Keith D. Robertson. “DNA Methyltransferases (DNMTs), DNA Damage Repair, and Cancer.” Advances in experimental medicine and biology 754 (2013): 3–29. PMC. Web.

[29] Kholodenko, Irina V., and Konstantin N. Yarygin. “Cellular Mechanisms of Liver Regeneration and Cell-Based Therapies of Liver Diseases.” BioMed Research International 2017 (2017): 8910821. PMC. Web.

[30] Kholodenko, Irina V., and Konstantin N. Yarygin. “Cellular Mechanisms of Liver Regeneration and Cell-Based Therapies of Liver Diseases.” BioMed Research International 2017 (2017): 8910821. PMC. Web.

[31] Koniaris, Leonidas G., Iain H. McKillop, Seymour I. Schwartz, and Teresa A. Zimmers. "Liver Regeneration." Journal of American College of Surgeons 197.4 (2003): 634-59. Web.

[32] Krebs, Christopher J. et al. “The KRAB Zinc Finger Protein RSL1 Modulates Sex-Biased Gene Expression in Liver and Adipose Tissue To Maintain Metabolic Homeostasis.” Molecular and Cellular Biology 34.2 (2014): 221–232. PMC. Web.

[33] Lee, J.-H., and D. G. Skalnik. "CpG-binding Protein (CXXC Finger Protein 1) Is a Component of the Mammalian Set1 Histone H3-Lys4 Methyltransferase Complex, the Analogue of the Yeast Set1/COMPASS Complex." Journal of Biological Chemistry 280.50 (2005): 41725-1731. Web.

[34] Lim, Derek H K, and Eamonn R. Maher. "DNA methylation: a form of epigenetic control of gene expression." The Obstetrician & Gynaecologist 12.1 (2010): 37-42. Web.

[35] Lonardo, A., C.d. Byrne, S.h. Caldwell, H. Cortez-Pinto, and G. Targher. "Global epidemiology of nonalcoholic fatty liver disease: Meta-analytic assessment of prevalence, incidence, and outcomes." Hepatology 64.4 (2016): 1388-389. Web.

[36] Mahadevan, Jyothi, and David G. Skalnik. "Efficient differentiation of murine embryonic stem cells requires the binding of CXXC finger protein 1 to DNA or methylated histone H3-Lys4." Gene 594.1 (2016): 1-9. Web.

[37] Mahadevan, Jyothi. The role of CFP1 in murine embryonic stem cell function and liver regeneration. Diss. Indiana U, 2015. N.p.: n.p., n.d. Print.

[38] Mariño-Ramírez, Leonardo et al. "Histone Structure and Nucleosome Stability." Expert review of proteomics 2.5 (2005): 719–729. PMC. Web.

[39] Milona, Alexandra et al. "The Normal Mechanisms of Pregnancy-Induced Liver Growth Are Not Maintained in Mice Lacking the Bile Acid Sensor Fxr." American Journal of Physiology - Gastrointestinal and Liver Physiology 298.2 (2010): G151–G158. PMC. Web.

[40] Nikoozad, Zahra, Mohammad Taghi Ghorbanian, and Arezou Rezaei. "Comparison of the Liver Function and Hepatic Specific Genes Expression in Cultured Mesenchymal Stem Cells and Hepatocytes." Iranian Journal of Basic Medical Sciences 17.1 (2014): 27–33. Print.

[41] Noakes, David E., Timothy J. Parkinson, and Gary C.W. England. Arthur's Veterinary Reproduction and Obstetrics. 9th ed. N.p.: Saunders Elsevier, 2009. Print.

[42] Noble, D. "Conrad Waddington and the origin of epigenetics." Journal of Experimental Biology 218.6 (2015): 816-18. Web.

[43] Ordog, T., S. A. Syed, Y. Hayashi, and D. T. Asuzu. "Epigenetics and chromatin dynamics: a review and a paradigm for functional disorders." Neurogastroenterology & Motility 24.12 (2012): 1054-068. Web.

[44] Peters, Antoine Hfm, and Dirk Schübeler. "Methylation of histones: playing memory with DNA." Current Opinion in Cell Biology 17.2 (2005): 230-38. Web.

[45] Phillips, Theresa. "The Role of Methylation in Gene Expression." Nature Education 1(1):116 Web.

[46] Puri, Puneet, and Arun J. Sanyal. "Nonalcoholic fatty liver disease: Definitions, risk factors, and workup." Clinical Liver Disease 1.4 (2012): 99-103. Web.

[47] Ress, Claudia, and Susanne Kaser. "Mechanisms of Intrahepatic Triglyceride Accumulation." World Journal of Gastroenterology 22.4 (2016): 1664–1673. PMC. Web.

[48] Riehle, Kimberly J. et al. "New Concepts in Liver Regeneration." Journal of gastroenterology and hepatology 26.Suppl 1 (2011): 203–212. PMC. Web.

[49] Scholzen, Thomas, and Johannes Gerdes. "The Ki-67 protein: From the known and the unknown." Journal of Cellular Physiology 182.3 (2000): 311-22. Web.

[50] Sharma, Mithun et al. "The Riddle of Nonalcoholic Fatty Liver Disease: Progression from Nonalcoholic Fatty Liver to Nonalcoholic Steatohepatitis." Journal of Clinical and Experimental Hepatology 5.2 (2015): 147–158. PMC. Web.

[51] Shin, Donghun, and Satdarshan Pal Singh Monga. "Cellular and Molecular Basis of Liver Development." Comprehensive Physiology 3.2 (2013): 799–815. PMC. Web.

[52] Stimpson, Kaitlin M, and Beth A Sullivan. "Histone H3K4 Methylation Keeps Centromeres Open for Business." The EMBO Journal 30.2 (2011): 233–234. PMC. Web.

[53] Tate, Courtney M., Jeong-Heon Lee, and David G. Skalnik. "CXXC Finger Protein 1 Contains Redundant Functional Domains That Support Embryonic Stem Cell Cytosine Methylation, Histone Methylation, and Differentiation." Molecular and Cellular Biology 29.14 (2009): 3817–3831. PMC. Web.

[54] Thomson, John P., Peter J. Skene, Jim Selfridge, Thomas Clouaire, Jacky Guy, Shaun Webb, Alastair R. W. Kerr, Aimée Deaton, Rob Andrews, Keith D. James, Daniel J. Turner, Robert Illingworth, and Adrian Bird. "CpG islands influence chromatin structure via the CpG-binding protein Cfp1." Nature 464.7291 (2010): 1082-086. Web.

[55] Tolman, Keith G, and Anthony S Dalpiaz. "Treatment of Non-Alcoholic Fatty Liver Disease." Therapeutics and Clinical Risk Management 3.6 (2007): 1153–1163. Print.

[56] Toshikuni, Nobuyuki, Mikihiro Tsutsumi, and Tomiyasu Arisawa. “Clinical Differences between Alcoholic Liver Disease and Nonalcoholic Fatty Liver Disease.” World Journal of Gastroenterology : WJG 20.26 (2014): 8393–8406. PMC. Web.

[57] Voo, K.S., D.L. Carlone, B.M. Jacobsen, A. Flodin, and D.G. Skalnik. 2000. Cloning of a mammalian transcriptional activator that binds unmethylated CpG motifs and shares a CXXC domain with DNA methyltransferase, human trithorax, and methyl-CpG binding domain protein 1. Molecular and cellular biology. 20:2108-2121.

[58] Waxman, D. J. "Sexual dimorphism of hepatic gene expression: novel biological role of KRAB zinc finger repressors revealed." Genes & Development 17.21 (2003): 2607-613. Web.

[59] Weisiger, Richard A. "Conjugated Hyperbilirubinemia." Background, Pathophysiology, Etiology. Ed. BS BS Anand. N.p., 11 Apr. 2017. Web.

[60] Weiskirchen, Ralf, and Frank Tacke. “Cellular and Molecular Functions of Hepatic Stellate Cells in Inflammatory Responses and Liver Immunology.” Hepatobiliary Surgery and Nutrition 3.6 (2014): 344–363. PMC. Web.

[61] Xu, Chao et al. “The Structural Basis for Selective Binding of Non-Methylated CpG Islands by the CFP1 CXXC Domain.” Nature Communications 2 (2011): 227–. PMC. Web.

[62] Zhang, Juanwen, Ying Zhao, Chengfu Xu, Yani Hong, Huanle Lu, Jianping Wu, and Yu Chen. "Association between serum free fatty acid levels and nonalcoholic fatty liver disease: a cross-sectional study." Scientific Reports 4.1 (2014): n. pag. Web.

[63] Zou, Yuhong, Qi Bao, Sudhanshu Kumar, Min Hu, Guo-Ying Wang, and Guoli Dai. "Four Waves of Hepatocyte Proliferation Linked with Three Waves of Hepatic Fat Accumulation during Partial Hepatectomy-Induced Liver Regeneration." PLoS ONE 7.2 (2012): n. pag. Web.